2010-05-25

Optimization and Correlation of the Penn State Model of Friction Stir Welding to Experimental Welds in 304L Stainless Steel

Devin Donaldson Furse
Brigham Young University - Provo

Optimization and Correlation of the Penn State Model of Friction Stir Welding to Experimental Welds in 304L Stainless Steel

Devin D. Furse

A thesis submitted to the faculty of
Brigham Young University
in partial fulfillment of the requirements for the degree of

Master of Science

Carl D. Sorensen, Chair
Tracy W. Nelson
Matthew R. Jones

Department of Mechanical Engineering

Brigham Young University

August 2010

ABSTRACT

Optimization and Correlation of the Penn State Model of Friction Stir Welding to Experimental Welds in 304L Stainless Steel

Devin D. Furse

Department of Mechanical Engineering

Master of Science

A numerical model of friction stir welding developed by T. DebRoy, R. Nandan, and others has been optimized to fit experimental data of eleven welds of 304L stainless steel at various weld feed rates and spindle speeds. Optimization was used to determine the values of five difficult-to-measure model parameters. The optimal parameter values were then correlated to the weld machine inputs. The mechanical efficiency and the coefficient of friction were not correlated with feed rate, spindle speed, or axial pressure. Tool slip was positively correlated with feed rate, negatively correlated with spindle speed, and not correlated with axial pressure. The heat partition factor was positively correlated with feed rate, negatively correlated with spindle speed, and negatively correlated with axial pressure. The heat transfer coefficient at the bottom face was positively correlated with feed rate, not correlated with spindle speed, and positively correlated with axial pressure.

The above welds were instrumented with thermocouples at the mid-plane of the workpiece. Recently acquired three-dimensional temperature data indicates that the two-dimensionally optimized model does not sufficiently capture the thermal profiles in all three directions. However, optimizing the model to fit the three-dimensional data does not yield acceptable results either. Several potential sources for model improvement are identified, primarily the modeling of heat transfer at the bottom surface. It is shown that using a spatially-variable thermal contact resistance approach is more theoretically justifiable and yields better temperature predictions.

Keywords: Devin Furse, DebRoy, modeling, friction stir welding, stainless steel

ACKNOWLEDGMENTS

I am indebted to many individuals for their assistance and support in pursuing and completing this thesis. Thank you to my wife, Megan; my parents, Darryl and Martha; my advisor, Carl Sorensen; the members of my committee, Tracy Nelson and Matthew Jones; and other associates, friends, and family members too numerous to mention.

This research was supported by the Center for Friction Stir Processing, an NSF Industry/University cooperative research center.

TABLE OF CONTENTS

LIST OF TABLES

LIST OF FIGURES

1 INTRODUCTION

1.1 Background

Friction stir welding (FSW) is a joining process originally developed at The Welding Institute in Cambridge, England [1]. In the process, a rotating tool is brought into contact with the workpiece(s), generating frictional heat and lapping the softened, plasticized material around the tool pin, as shown in Figure 1-1. FSW is a solid-state process, meaning that the workpiece temperature stays below the melting point. This results in superior mechanical properties when compared to traditional fusion welds. Other advantages over fusion welds are low workpiece distortion and less porosity.

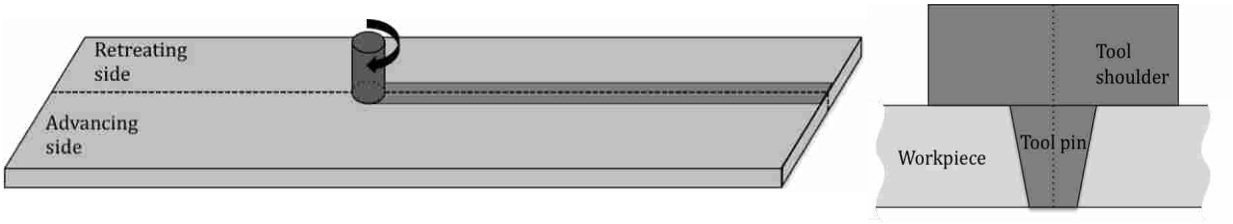

Figure 1-1: Depiction of friction stir welding.

In the early stages, FSW was primarily limited to aluminum alloys. However, with improvements in tool materials and design, higher melting point materials such as steels and Nickel-based alloys are now able to be friction stir welded [2].

Various analytical and numerical models of FSW have been widely published and reported on, including a model developed by T. DebRoy and others at the Pennsylvania State University [3]. Although use of the Penn State model to predict weld behavior in stainless steel has been reported in the literature, there was limited correlation of model predictions to experimental measurements [4].

1.2 Objective

The purpose of this study is primarily to improve the Penn State model's predicted thermal profiles of 304L stainless steel. This is done by optimization techniques where key difficult-to-measure model parameters are adjusted to produce thermal profiles that match measured temperatures. By optimizing over many different welds, the model parameters may be represented as functions of feed rate, spindle speed, and axial pressure, rather than as constants. This leads to more reliable model predictions of temperature.

1.3 About this thesis

This thesis consists of a collection of three papers that have either been published or have been submitted for publication. The first paper was published in the Fourth International Conference on Computational Methods and Experiments in Materials Characterisation held at the Wessex Institute of Technology in Ashurst, UK [5]. It presents a method of using optimization techniques to determine the values of difficult-to-measure parameters in the Penn State model of friction stir welding. The second paper builds off of the first by performing a regression analysis on the optimized welds, allowing the model parameters to be expressed as functions of weld machine variables (feed rate, spindle speed, and axial pressure). The third

paper builds off of the previous two and presents experimental results from a three-dimensionally instrumented plate. It examines whether the model improvements based on optimizing mid-plane temperatures results in acceptable three-dimensional temperature profiles, and whether three-dimensional optimization results in model predictions that fit actual measurements.

2 OPTIMIZATION OF A NUMERICAL MODEL OF THREE-DIMENSIONAL HEAT TRANSFER DURING FRICTION STIR WELDING OF 304L STAINLESS STEEL

2.1 Abstract

A numerical model of friction stir welding has been optimized to fit experimental data of three welds of 304L stainless steel at various weld velocities and spindle speeds. Optimization was used to determine the values of six model parameters that describe phenomena during the welding process. The parameter values were then compared to each other and to the default values. Predicted tool slip was determined to vary significantly with differing weld conditions. The coefficient of friction was also shown to vary. The mechanical efficiency of the three welds was predicted to range between 0.80 – 0.90. Optimization of additional welds is suggested so that correlations of the model parameters to weld velocity and spindle speed can be determined.

2.2 Introduction

Friction stir welding (FSW) is a solid state welding process in which a rotating tool generates heat along the joint interface, resulting in the flow of plasticized material around the tool. Since 1991, when FSW was developed at TWI [1], many models (both analytical and numerical) have been documented. An effective model of FSW can be a valuable predictive tool, allowing researchers to develop the process much more rapidly than could be accomplished through experiments only. Also, a good model of FSW can help researchers come to a better understanding of how the process works.

In this paper, a model of friction stir welding developed by T. DebRoy, R. Nandan, and others [4,6,7] is explored. The use of the model, which will be referred to as the Penn State model, requires the user to input six parameters that describe various aspects of the process—a slip constant, a friction constant, a viscous dissipation constant, a mechanical efficiency factor, a "fraction of heat entering the workpiece" factor, and a constant for the heat transfer at the bottom face. These parameters can be difficult or near impossible to measure, so an optimization approach is used to determine the parameter values that will "best fit" the model to experimental data. If the Penn State model is to be used to predict weld behavior, these parameters must be 1) bounded with some confidence and 2) known to what extent they vary with weld velocity and spindle speed. This paper will explore both issues.

2.3 Description of optimization approach

2.3.1 Experimental data

The data used to optimize the Penn State model comes from an unpublished work of 11 welds of varying rotational speeds and feed rates performed by Owen [8]. Each weld was performed on a 304L stainless steel workpiece with dimensions 60.96 cm x 20.32 cm x 0.635 cm. The tool used for the welds was a MegaStir Technologies™ E44016 Polycrystalline Cubic Boron Nitride (PCBN) tool. For reference, the welds are given corresponding numbers in Table 2-1.

The majority of welds will be used in determining the correlation, if one exists, of the model parameters to the weld conditions given. The remaining welds will be used to test the accuracy of the correlation.

Table 2-1: Welds performed by Owen [8] and their intended use.

Weld No.	*Spindle Speed (rpm)*	*Feed Rate (mm/s)*	*Used to determine correlation*	*Used to validate correlation*
1	300	0.423	X	
2	300	0.847	X	
3	300	1.693		X
4	300	2.54	X	
5	400	0.847		X
6	400	1.693	X	
7	400	2.54		X
8	500	0.423	X	
9	500	0.847	X	
10	500	1.693		X
11	500	2.54	X	

Model accuracy is assessed by comparing the predicted temperatures at specific locations in the workpiece with those obtained experimentally. Each workpiece was instrumented with 16 thermocouples distributed as shown in Figure 2-1, where the y position indicated is the distance from the weld centerline (positive y is the retreating side). All thermocouples were placed at a depth of z = 3.4 mm. Spindle torque and forces in all three directions were simultaneously recorded. The most interior thermocouples were placed very close to the stir zone of the tool, but were not displaced during the weld.

By using two thermocouples at identical y locations (but different x locations), Owen was able to show a repeatability error of only ~25 °C [8]. This indicated that the steady-state assumption used in numerical models of friction stir welding was suitable for the welds he performed. The repeatability error is also useful for establishing an acceptable level of model accuracy. The model error is given by

$$E = \sum_{i=1}^{n} \left(T_{i,measured} - T_{i,predicted} \right)^2 \tag{2-1}$$

where $T_{i,measured}$ is the peak temperature measured at location i and $T_{i,predicted}$ is the peak temperature predicted by the model at the same location. Thus, using eqn (2-1) for n monitoring locations, the model error is not expected to be less than $E = 25^2 n$ or $E = 625n$.

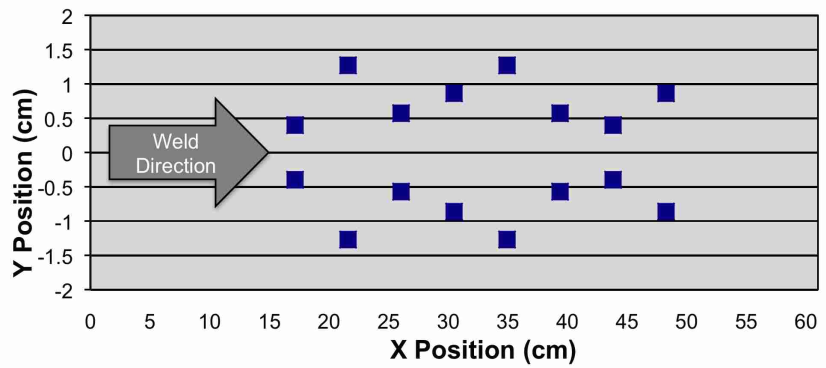

Figure 2-1: Locations of thermocouples in workpiece (not to scale) as given in [8].

2.3.2 Optimization routine

Optimization of the Penn State model is accomplished through the software package OptdesX. The objective of the optimization was to minimize the error function given in eqn (2-1) by changing the six model parameters previously mentioned. Six monitoring locations are used, with y values corresponding to the thermocouples at -1.27, -0.86, -0.40, 0.40, 0.86, and 1.27 cm. The optimization does not require any constraining functions. Since it is likely that more than one combination of model parameters may yield similar results – in other words, the solution may not be unique – the default values for 304L stainless steel (see Table 2-2) are used as the initial starting points for each optimization routine. This helps to ensure that each search begins by looking for a minimum in the same area. The generalized reduced gradient (GRG) algorithm within OptdesX was the search algorithm used.

A shell file written for OptdesX controls the flow of information in the process by calculating the model error and updating the values of the analysis variables as directed by OptdesX. The shell file serves as a link between the analysis engine (the Penn State model) and the optimization engine (OptdesX). In this approach, there is not one optimization problem, but rather seven optimization problems, where the welds used for correlation (see Table 2-1) are optimized. The remaining welds will be used to validate the correlation obtained.

2.4 Preliminary results

The optimal values for the six model parameters have been determined for Welds No. 1, 4, and 9. They are shown below in Table 2-2. For Weld No. 1, the default parameters led to a model error of E = 116,260, which by eqn (1) and for six monitoring locations corresponds to an average location error of 139 °C. Optimization reduced the error to 3,040 (22.5 °C) – slightly less than the minimum expected value of 3,750 (25 °C). Similarly, Welds No. 4 and No. 9 began with high model errors at the default position (154 °C and 113 °C, respectively), and ended with lower errors at the optimum position (44 °C and 30 °C). In each case, the model initially under-predicted the temperatures at all locations, but especially those closest to the weld.

Table 2-2: Optimal coefficient values for the welds tested.

Parameter	*Default Values*	*Optimal Values for Welds*		
		No. 1	*No. 4*	*No. 9*
Slip constant, δ_0	2.0	1.97	3.18	0.77
Friction constant, μ_0	0.45	0.50	0.58	0.46
Viscous dissipation constant, β	0.005	0.005	0.005	0.005
Mechanical efficiency, η	0.8	0.92	0.98	0.8
Fraction of heat entering workpiece, f	0.41	0.584	0.568	0.45
Heat transfer constant, h_0 (cal/cm^2-s-K$^{1.25}$)	0.004	0.0037	0.0041	0.002

Plotting the predicted peak temperatures at the specified monitoring locations against the data obtained experimentally shows that the model is fairly accurate (see Figure 2-2). Welds No.

1 and 9 were much hotter than Weld No. 4. This is due to the feed rate in Weld No. 4 being six times higher than in Weld No. 1 and three times higher than in Weld No. 9.

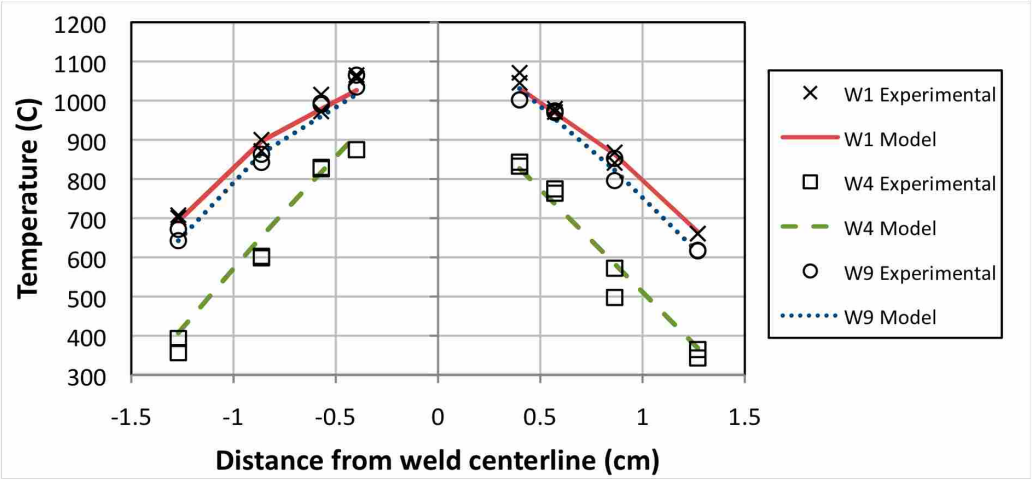

Figure 2-2: Peak temperatures in Weld Nos. 1, 4, and 9.

2.4.1 Slip constant

Slip at the tool-workpiece interface is modelled according to

$$\delta = 1 - \exp\left\{-\delta_0 \frac{\omega}{\omega_0} \frac{r}{R_S}\right\} \tag{2-2}$$

where δ is the fraction of slip, ω is the rotational speed of the tool, ω_0 is a reference value of rotational speed, r is the distance from the tool axis, and R_S is the radius of the tool shoulder. The constant δ_0 is the user-adjustable parameter of interest. Thus, the fraction of slip throughout the tool for the welds studied is distributed according to Figure 2-3. The default value ($\delta_0 = 2.0$) seemed to match closely with the optimal value of 1.97 for Weld No. 1, whereas Weld No. 9 had a significantly lower fraction of slip. This indicates that more sticking occurs at higher spindle speeds, which is a result that was not expected. Further work will demonstrate whether this is a

consistent result. Also, the optimal value of slip for Weld No. 4 indicates that higher feed rates may also increase the amount of sticking.

2.4.2 Friction constant

The optimal friction constant for Weld No. 1, $\mu_0 = 0.5$, was higher than the value chosen by Nandan et al for mild steel [6]. They chose $\mu_0 = 0.4$, and showed that in their case, adjusting the friction constant between 0.3 to 0.5 affected the peak temperature in the plate by about 100 K. Since Owen showed, as mentioned in Section 2.3.1, that the average error in thermocouple measurement was 25 K, a difference of 100 K is fairly significant.

The friction constant is used to scale the coefficient of friction according to

$$\mu = \mu_0 \exp\{-\lambda\delta\omega r\} \tag{2-3}$$

where λ is a constant equal to 1 s/m. Since the coefficient of friction is function of two user-adjustable parameters (δ and μ_0), each weld studied had a slightly different shape and scale for the distribution for friction. The friction coefficient for the welds studied is shown in Figure 2-3. From the distributions of slip and friction shown, it appears that there is a correlation between the two parameters: the higher the friction coefficient, the more slip is present. It is unknown if this relationship only applies to the model, or if it represents real phenomena during FSW of 304L stainless steel.

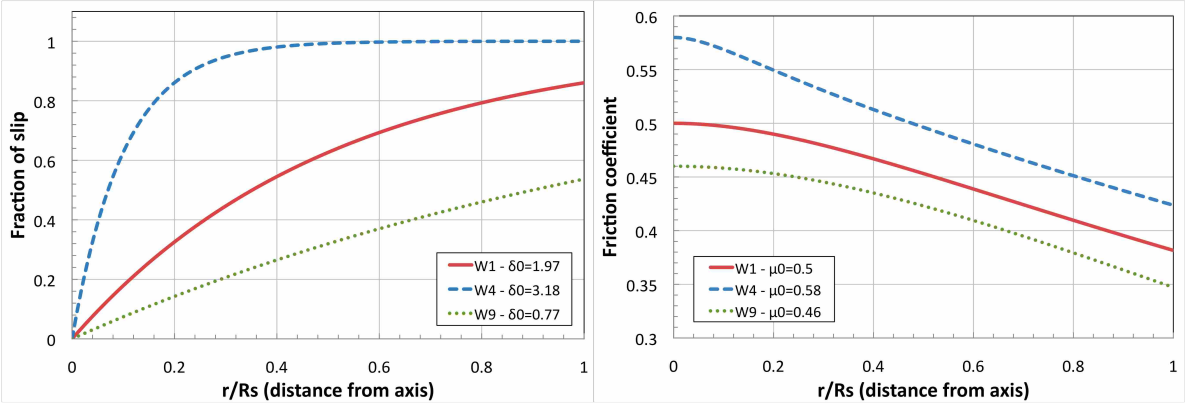

Figure 2-3: Fraction of slip and coefficient of friction used in the optimization of Welds No. 1, 4, and 9.

2.4.3 Viscous dissipation constant

The viscous dissipation constant β is used in determining the heat generated from plastic deformation, S_b, by the equation $S_b = \beta\mu\Phi$. The function Φ is defined as

$$\Phi = 2\left[\left(\frac{\partial u_1}{\partial x_1}\right)^2 + \left(\frac{\partial u_2}{\partial x_2}\right)^2 + \left(\frac{\partial u_3}{\partial x_3}\right)^2\right] + \left(\frac{\partial u_1}{\partial x_2} + \frac{\partial u_2}{\partial x_1}\right)^2 + \left(\frac{\partial u_1}{\partial x_3} + \frac{\partial u_3}{\partial x_1}\right)^2 + \left(\frac{\partial u_2}{\partial x_3} + \frac{\partial u_3}{\partial x_2}\right)^2 \tag{2-4}$$

Optimization showed that the temperature profile of the workpiece was not sensitive to changes in β. This was anticipated since the heat generated due to viscous dissipation is fairly small. Yet, as Nandan *et al* conclude, without this term, the temperature profile does not vary with respect to changes in viscosity [6].

2.4.4 Mechanical efficiency

The mechanical efficiency, η, represents the fraction of workpiece deformation that generates heat. It is used in heat generation at the tool-workpiece interface, S_i, according to

$$S_i = \sum\left[(1-\delta)\eta\tau + \delta\mu P_N\right](\omega r - U_1 \sin\theta)\frac{A_r}{V} \tag{2-5}$$

where τ is the shear stress at yielding, P_N is the normal pressure, θ is the tilt angle of the tool, U_1 is the weld velocity or feed rate, A_r is the discrete area in contact with the tool, and V is the discrete volume enclosing the area A_r.

The model is predicting that mechanical efficiency diminishes as the rotational velocity increases. The change in η from Weld No. 4 to No. 9 was quite significant – a decrease of about 18 percent. Optimizing the other welds will clarify whether this change is solely due to changing the rotational speed or if other factors are contributing.

2.4.5 Fraction of heat entering workpiece

The fraction of heat entering the workpiece, f, is a parameter that when combined with the mechanical efficiency describes the percentage of power from the FSW machine that is converted into heat in the workpiece. Although the user is free to choose any value for f, Nandan et al [6] suggest using the following equation, which comes from steady-state one dimensional heat transfer from a point source located in the interface of two dissimilar materials at the same temperature [9].

$$f = \frac{J_W}{J_W + J_T} = \frac{1}{1 + \sqrt{(k\rho c)_T / (k\rho c)_W}} \tag{2-6}$$

where J is the heat flux and the subscript W and T represents the workpiece and the tool respectively. Using eqn (2-6) for a PCBN tool and 304L stainless workpiece, f is calculated to be ~ 40 percent, which is the value chosen by Nandan et al in their study of stainless steel [4]. This is comparable to the optimal values for the welds optimized so far, especially Weld No. 9 (f = 0.45). The welds with slower rotational velocities predicted more heat entering the workpiece.

The fraction of heat entering the workpiece seems to be calibrated low in the model. Eqn (2-6) assumes that both the tool and the workpiece are at the same temperature, a condition

perhaps true towards the end of the plunge phase, but not during the weld, when the tool is moving into much cooler workpiece material. Shercliff and Colegrove state that heat lost into the tool is typically on the order of 10% or less [3]. When combined with the mechanical efficiency, the total predicted amount of power from the machinery entering the workpiece is ηf, which in the welds studied is only 0.35 – 0.55. Chao *et al* showed that this "heat efficiency" during FSW of aluminum was about 95 percent, which is much higher than the heat efficiency of traditional fusion welding (60-80%) [10]. However, they noted that the energy in FSW is converted from mechanical energy to heat and deformation, so that the term "heat efficiency" is not quite the same. It is unknown why the Penn State model predicts such a low fraction of heat entering the workpiece.

2.4.6 Heat transfer coefficient at bottom face

The heat transfer at the bottom surface (z = 0) is modeled as Newtonian cooling under natural convection:

$$k\left.\frac{\partial T}{\partial z}\right|_{bottom} = h\left(T - T_a\right) \tag{2-7}$$

where T_a is the ambient temperature. The coefficient h is given by $h = h_0(T - T_a)^{0.25}$ where h_0 is our unknown parameter with units equal to cal/cm^2-s-K$^{1.25}$ [11]. Thus, the heat transfer coefficient at the bottom face is a function of the temperature at the face and the constant h_0 given by the user. The optimal h_b for Welds No. 1 and 4 stayed close to the default value (h_0 = 0.004 cal/cm^2-s-K$^{1.25}$), corresponding to an h value of about 900 W/m^2-K under the tool. Weld No. 9 however, had an h_0 = 0.002 cal/cm^2-s-K$^{1.25}$.

Shercliff and Colegrove have suggested using a spatially variable (rather than temperature variable) heat transfer coefficient due to the different conditions of contact

resistance between the workpiece and the backing plate [3]. Below and behind the tool, the contact resistance is low, due to the downward force. Away from the tool, however, the contact resistance is high; the clamping points can be neglected. Thus, the heat transfer constant h_0 should not be a function of weld velocity or spindle speed.

2.5 Conclusion

A method for determining previously unknown parameters in the Penn State model through optimization techniques has been discussed. Results were shown to lead to accurate predictions of workpiece thermal profiles. Because the model is still under development, this method will be helpful in identifying discrepancies between the model and experimental data. It is probably too early to make any definitive statements on how the model parameters should be adjusted with regards to weld velocity and spindle speed. Likewise, although the optimized parameters correspond to material behavior during friction stir welding, statements on the characteristics of 304L stainless steel during FSW would be premature.

Although the use of optimization techniques is a roundabout way of determining the values of model parameters, it has been shown to yield reliable thermal profiles of the workpiece. Optimizing the other welds will allow more concrete statements to be made about model performance and predictions. In addition, correlations of the model parameters will allow the model to be used in a more predictive way, and it will yield further insight into the behavior of 304L stainless steel during friction stir welding.

3 CORRELATION OF A NUMERICAL MODEL OF FRICTION STIR WELDING OF 304L STAINLESS STEEL TO EXPERIMENTAL THERMAL PROFILES

3.1 Abstract

A numerical model of friction stir welding developed by T. DebRoy, R. Nandan, and others has been optimized to fit experimental data of eleven welds of 304L stainless steel at various weld feed rates and spindle speeds. Optimization was used to determine the values of five difficult-to-measure model parameters. The optimal parameter values were correlated to the weld machine inputs. The mechanical efficiency and the coefficient of friction were not correlated with feed rate or spindle speed. Tool slip was positively correlated with feed rate and negatively correlated with spindle speed. The heat partition factor was positively correlated with feed rate and negatively correlated with spindle speed. The heat transfer coefficient at the bottom face was positively correlated with feed rate and not correlated with spindle speed.

3.2 Introduction

Friction stir welding (FSW) is a solid state welding process in which a rotating tool generates heat along the joint interface, resulting in the flow of plasticized material around the tool. Since 1991, when FSW was developed at TWI [1], many models (both analytical and numerical) have been documented [3]. An effective model of FSW can be a valuable tool, allowing researchers to predict weld temperatures and forces much more quickly than through

experimentation. In addition, a good model of FSW can help researchers come to a better understanding of how the process works.

In this paper, a model of friction stir welding developed by T. DebRoy, R. Nandan, and others [4,6,7] is explored. The accuracy of this model, which will be referred to as the Penn State model, is highly dependent on five difficult-to-measure parameters that describe various aspects of the process. These parameters are 1) η, a fraction relating how much energy from workpiece shear is converted to heat, 2) δ_0, a scaling factor for slip at the tool-workpiece interface, 3) μ_0, a scaling factor for the coefficient of friction at the tool-workpiece interface, 4) f, a heat partition factor relating the fraction of heat entering the workpiece (as opposed to the tool), and 5) h_0, a scaling factor for the heat transfer coefficient at the bottom face of the plate. Although there are default values for each of these parameters, it is suggested that the model accuracy may be improved. Therefore, an optimization approach is used to determine the parameter values that match the model's predicted temperatures to those obtained experimentally. Once the optimal parameter values have been determined for each weld, a regression model is created for each parameter to predict the parameter values in terms of feed rate and/or spindle speed.

3.3 Description of optimization approach

3.3.1 Experimental data

The data used to optimize the Penn State model comes from an unpublished work of 11 welds of varying rotational speeds and feed rates performed by Owen [8]. Each weld was performed on a 304L stainless steel workpiece with dimensions 60.96 cm x 20.32 cm x 0.635 cm. The tool used for the welds was a MegaStir Technologies™ E44016 Polycrystalline Cubic

Boron Nitride (PCBN) tool. For reference, the welds are given corresponding numbers in Figure 3-1.

The majority of welds (7) are used in creating a regression of the model parameters to the weld conditions (feed rate and spindle speed). The four remaining welds are used to determine whether the regression model is valid.

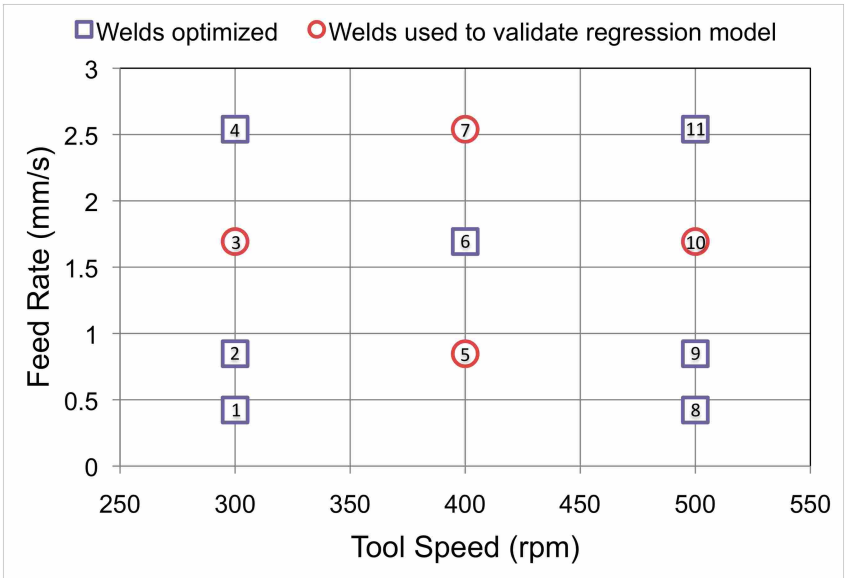

Figure 3-1: Welds used in the correlation study, numbered for reference.

The model error, E, is assessed by comparing the predicted temperatures at specific locations in the workpiece with those obtained experimentally, as in eqn (3-1).

$$E = \sum_{i=1}^{n} \left(T_{i,measured} - T_{i,predicted} \right)^2 \tag{3-1}$$

Furse and Sorensen [5] had previously calculated the model error using only the peak temperatures at a given distances from the weld centerline. This led to accurate temperature profiles in the y direction, but inaccurate temperature profiles in the x direction. Ideally, the model would calculate error based on temperatures in all three directions; however, this data is

not currently available to the authors for the wide range of spindle speeds and feed rates studied here. The locations used to compare temperatures are shown in Figure 3-2 below. All these points are located at the mid-plane (z = 3.4 mm). The original temperature data captures temperature over time. This data is transformed into the spatial dimension by calculating the thermocouple's relative x distance from the tool.

Using two thermocouples at identical y locations but different x locations, Owen calculated a repeatability error of approximately 25 °C in his welds [8]. This indicated that the steady-state assumption used in numerical models of friction stir welding was suitable for the welds he performed. The repeatability error is also useful for establishing an acceptable level of model accuracy. Using eqn (3-1) for the 42 monitoring locations from Figure 3-2 and an average repeatability error of 25 °C, the model error is not expected to be less than $E = 25^2(42)$ or $E = 26{,}250$.

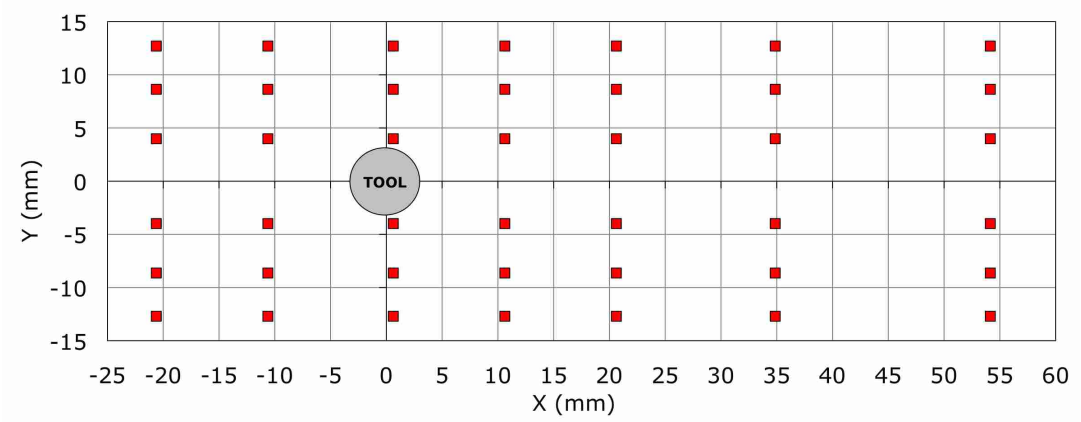

Figure 3-2: The 42 positions at which the model error *E* is calculated. All positions lie on the z = 3.4mm plane. Tool is traveling to the left.

3.3.2 Optimization routine

Optimization of the Penn State model is accomplished through the software package OptdesX. The objective of the optimization is to minimize the error function given in eqn (3-1) by changing the values of the five model parameters previously mentioned. The optimization

does not require any constraining functions. Since it is possible that the solution may not be unique (i.e. more than one combination of model parameters may yield similar minima), the default values for 304L stainless steel (see Table 3-1) are used as the initial starting points for each optimization routine. This helps to ensure that each search begins by looking for a minimum in the same area. The GRG algorithm within OptdesX was the search algorithm used.

A shell file written for OptdesX controls the flow of information in the process by calculating the model error and updating the values of the analysis variables as directed by OptdesX. The shell file serves as a link between the analysis engine (the Penn State model) and the optimization engine (OptdesX).

3.3.3 Regression analysis

All eleven welds are optimized, and the seven welds indicated in Figure 3-1 are used to form a regression model. The four welds remaining welds are also optimized in order to validate the regression model. A valid regression model meets two criteria: 1) The difference between the optimal parameter values and the predicted parameter values is small, and 2) The model error using the predicted parameter values is lower than using the default parameter values.

The regression models for the model parameters are constructed and analyzed via the Standard Least Squares method in the statistical software package JMP. The general procedure outlined in [12] is followed, where a full factorial regression model is constructed first, and is then updated by eliminating the statistically insignificant terms and reconstructing the regression model.

3.4 Results

The optimal values for the five model parameters have been determined for all welds. They are shown below in Table 3-1. The corresponding model error is also shown for both the default and optimal model parameters. As expected, the optimization routine significantly reduced the model error. In Weld No. 1 for example, the default parameters led to a model error of E = 532,300, which by eqn (3-1) and for 42 monitoring locations corresponds to an average location error of 113 °C. Optimization reduced the model error to E = 30,300 (26.9 °C) – close to the minimum expected value of 25 °C due to uncertainty. There was significant reduction of error in most of the other welds as well.

Table 3-1: Parameter values for the optimized welds, including the beginning (default) model error and the ending (optimal) model error.

Weld No	Spindle Speed (rpm)	Feed Rate (mm/s)	Axial Pressure (MPa)	Default Model Error	Optimal Model Error	Tool Slip Parameter (δ_0)	Friction Coefficient Parameter (μ_0)	Heat Transfer Parameter (h_0) ($cal/cm^2sK^{1.25}$)	Mechanical Efficiency Parameter (η)	Heat Partition Parameter (f)
					Default values:	2.0	0.45	0.004	0.8	0.41
1	300	0.423	57.9	532,300	30,300	6.62	0.412	0.00203	0.754	0.447
2	300	0.847	144.4	230,600	91,100	3.76	0.451	0.00286	0.805	0.404
3	300	1.693	93.77	328,800	70,200	5.15	0.474	0.00486	0.926	0.705
4	300	2.54	126.2	185,100	29,000	6.57	0.463	0.00713	0.839	0.625
5	400	0.847	96.4	119,500	93,400	2.45	0.448	0.00317	0.789	0.387
6	400	1.693	127.4	160,300	59,200	6.37	0.457	0.00479	0.785	0.448
7	400	2.54	113	238,500	37,400	7.35	0.463	0.00658	0.807	0.607
8	500	0.423	66.9	600,800	31,200	1.14	0.438	0.00168	0.790	0.364
9	500	0.847	69.5	240,800	56,000	3.17	0.454	0.00275	0.800	0.464
10	500	1.693	120.7	90,000	67,700	3.28	0.449	0.00492	0.800	0.431
11	500	2.54	157.5	100,800	41,000	3.94	0.447	0.00664	0.798	0.432

In general, the default model parameters led to lower than actual temperatures close to the tool and faster than actual cooling rates. Both results can be seen in Figure 3-3 below, in

which the actual temperature contours are overlaid on the Penn State model's predicted temperature contours. Optimization ameliorated both of these issues.

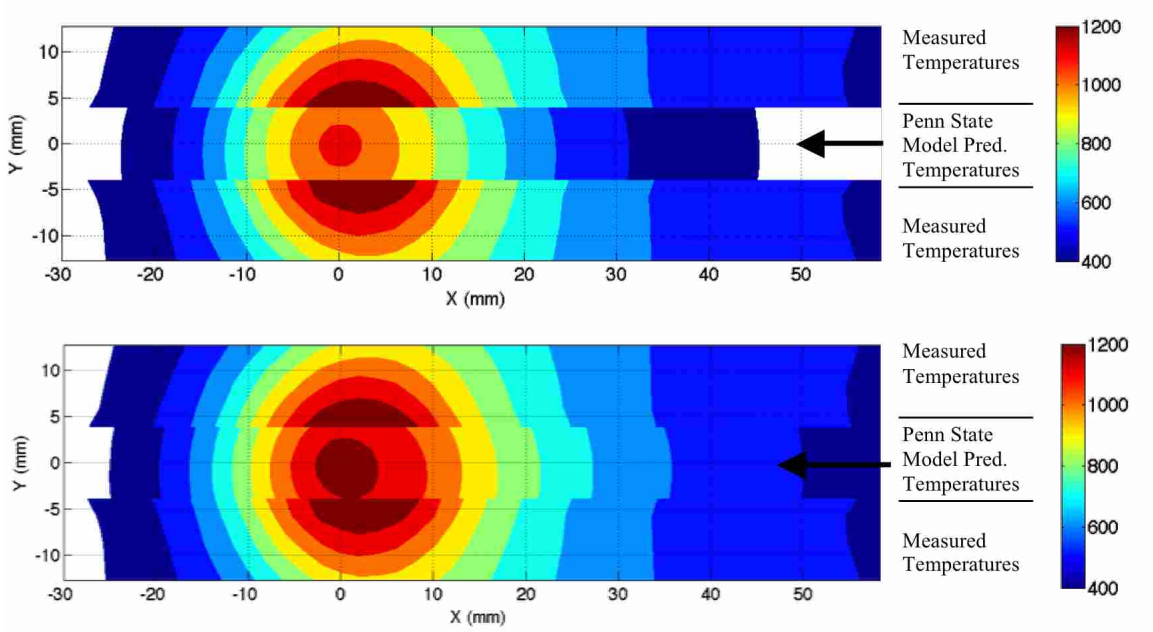

Figure 3-3: Weld No. 1 measured and predicted temperature contours (K) on the plane z = 3.4 mm for the default parameter values (top) and the optimal parameter values (bottom).

3.4.1 Mechanical efficiency

The parameter, η, or "mechanical efficiency," is the fraction of workpiece shear energy at the tool-workpiece interface that is converted to heat. It only applies to the interfacial heat generation due to sticking friction. The total interfacial heat generation of a discrete volume, S_i, is given by eqn (2-5).

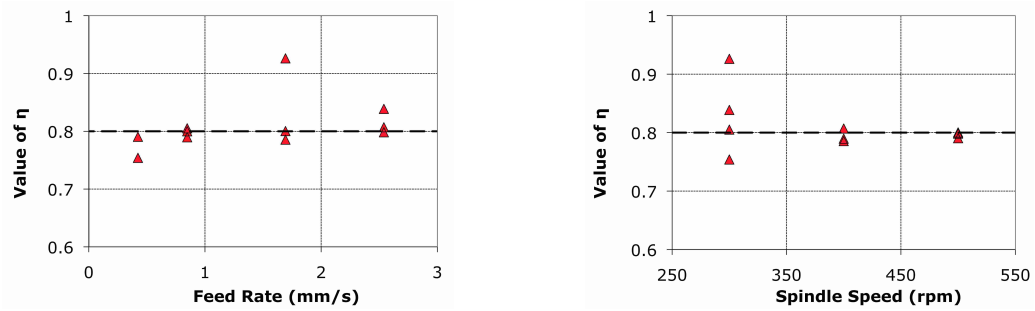

Figure 3-4: Optimal values of η plotted against weld inputs. Dashed line is default value.

Figure 3-4 plots the optimal values of η against the weld inputs, and by inspection, it appears that the mechanical efficiency is not correlated to either of them. Apart from a few outliers, the optimal value stays pretty close to the default value of 0.8. Thus, a regression model for η appears unnecessary. This result suggests that the fraction of plastic deformation converted to heat in FSW is constant for all applicable feed rates and spindle speeds.

3.4.2 Slip constant

Slip at the tool-workpiece interface is modeled according to eqn (2-2), where the scaling factor δ_0 is the user-adjustable parameter of interest. Figure 3-5 shows the values obtained via optimization as functions of the weld inputs.

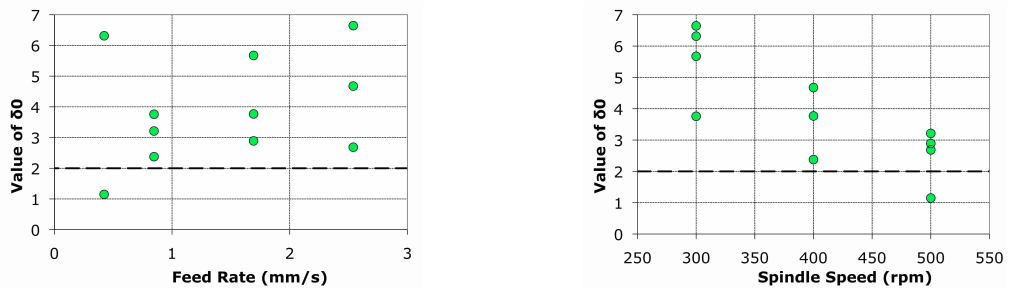

Figure 3-5: Optimal values of δ_0 plotted against weld inputs. Dashed line is default value.

Firstly, by Figure 3-5 it seems that the default value of $\delta_0 = 2.0$ is inappropriate, considering that the average optimal value is $\delta_0 = 4.53$. The parameter δ_0 is positively correlated with feed rate and negatively correlated with spindle speed. The regression equation for δ_0 is shown in eqn (3-2), and the actual vs. predicted plot for this regression model is shown in Figure 3-6. Note that the feed rate (*FR)* and the spindle speed (*SS*) in eqn (3-2) have units of mm/s and rpm, respectively.

$$\delta_0 = 9.1188 + (0.8973)FR - (0.0145)SS \tag{3-2}$$

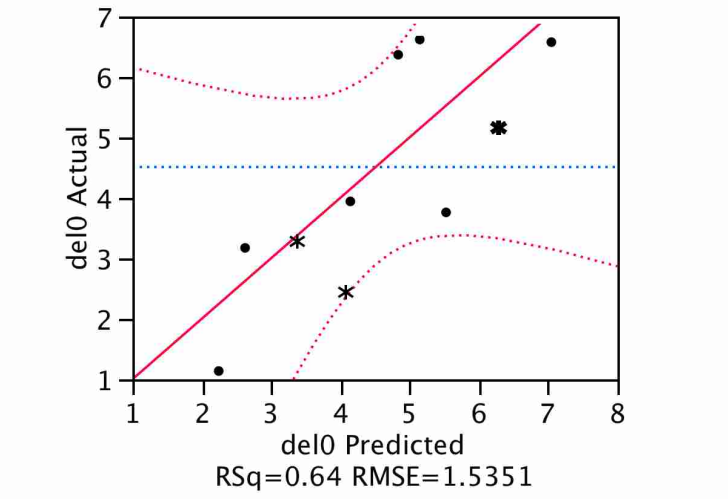

Figure 3-6: δ_0 regression model. Welds not used denoted by *.

The fact that the dashed 95% confidence boundaries in Figure 3-6 do not cross the horizontal dashed line (the mean value) indicate that this model is not statistically significant to 95% confidence. This unwelcome result is primarily due a low signal-to-noise ratio. The relatively small number of observations (seven) leaves only four degrees of freedom for error after constructing the regression model. However, the welds not used to construct the regression model do appear to validate the use of this model. In the absence of a better alternative, using the regression model is preferable to using the mean value (4.51) or the default value (2.0).

The regression model suggests that more sticking occurs at higher spindle speeds and lower feed rates. High spindle speed, low feed rate welds, because they run at higher workpiece temperatures, have been described as "hot" welds, with lower torques and forces due to material softening. Thus, the results here suggest that low force, "hot" welds are governed more by sticking friction, whereas high force, "cold" welds are governed more by slipping friction.

3.4.3 Friction coefficient

The friction coefficient parameter of interest, μ_0, is used in scaling the coefficient of friction, μ, according to eqn (2-3). From Figure 3-7, it appears that μ_0 is not correlated to any of the weld parameters. Throughout each optimization, μ_0 stayed very close to the default value of $\mu_0 = 0.45$. Thus, a regression model is not necessary for this parameter, and it is recommended to continue to use the default value. This result suggests that the coefficient of friction is not sensitive to changes in feed rate or spindle speed.

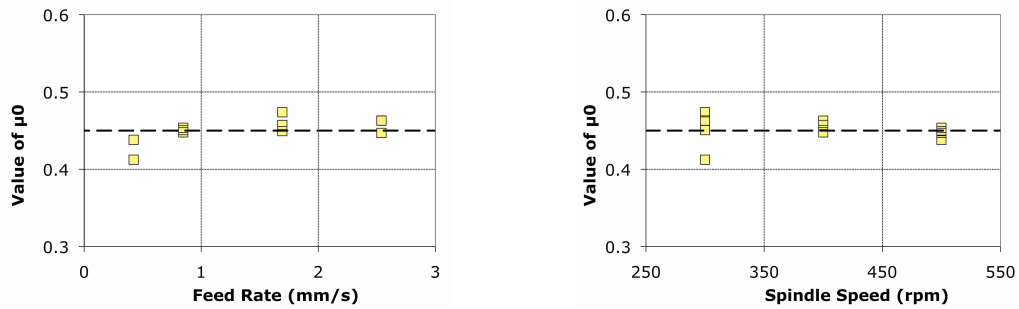

Figure 3-7: Optimal values of μ_0 plotted against weld inputs. Dashed line is default value.

3.4.4 Heat partition factor

The heat partition factor, *f*, is a parameter that indicates the fraction of interfacial heat generation, S_i, that enters the workpiece. Although the user is free to choose any value for *f*, Nandan et al [4] suggest using eqn (2-6), which comes from steady-state one dimensional heat transfer from a point source located in the interface of two dissimilar materials at the same temperature.

Using eqn (2-6) for a PCBN tool and 304L stainless workpiece, *f* is calculated to be ~ 40 percent, which is the value chosen by Nandan et al in their study of stainless steel [4]. The assumption that both the tool and the workpiece are at the same temperature is a condition

perhaps true when the tool is stationary, but during the weld, the tool is always moving into much cooler workpiece material. Thus, the higher values for *f* obtained through optimization are not unexpected, and, as Figure 3-8 confirms, higher feed rates should result in more heat partitioned to the workpiece.

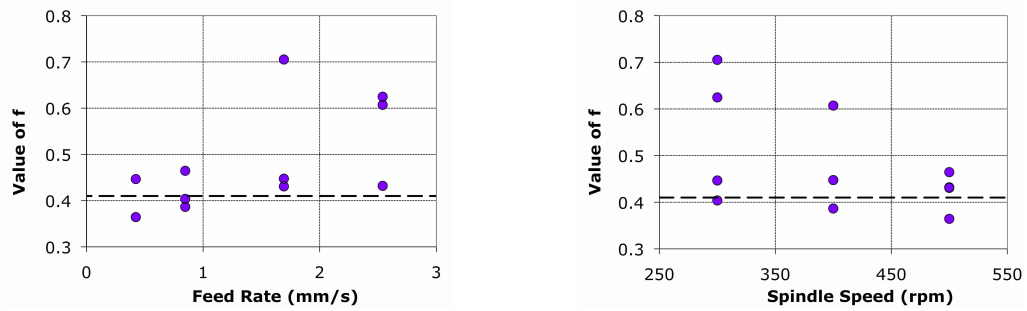

Figure 3-8: Optimal values of *f* plotted against weld inputs. Dashed line is default value.

The heat partition factor appears to be positively correlated with feed rate and negatively correlated with spindle speed. This result is similar to δ_0 in that for "hot" welds, *f* is low, and for "cold" welds, *f* is higher – in some cases, nearly two times higher. The regression equation for *f*, eqn (3-3), includes coefficients for both terms, where the feed rate (*FR*) and the spindle speed (*SS*) have units of mm/s and rpm respectively.

$$f = 0.5245 + (0.055)FR - (3.57 \times 10^{-4})SS \tag{3-3}$$

The actual by predicted plot for eqn (3-3) is given in Figure 3-9. As with the tool slip parameter, δ_0, the regression model for *f* is not statistically significant to the 95% confidence level. However, using this model is clearly superior to using the mean value (0.46) or the default value (0.41) when one examines that the four welds not used to create the regression model have optimal *f* values that suggest a higher slope than the regression model.

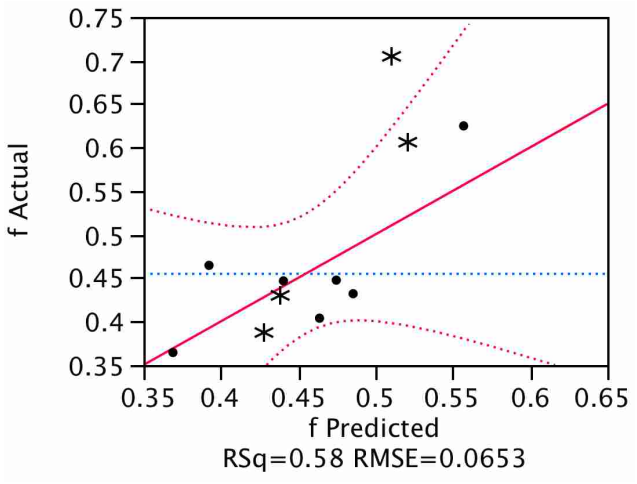

Figure 3-9: *f* regression model. Welds not used denoted by *.

3.4.5 Heat transfer coefficient

The heat transfer at the bottom surface ($z = 0$) is modeled as Newtonian, convective heat transfer via eqn (2-7). The "convection" coefficient h is given by

$$h = h_0\left(T - T_a\right)^{0.25} \tag{3-4}$$

where h_0 is the parameter of interest with units equal to cal/cm^2-s-K$^{1.25}$ [11]. Thus, the heat transfer coefficient at the bottom face is solely a function of the temperature at the face and the h_0 parameter supplied by the user.

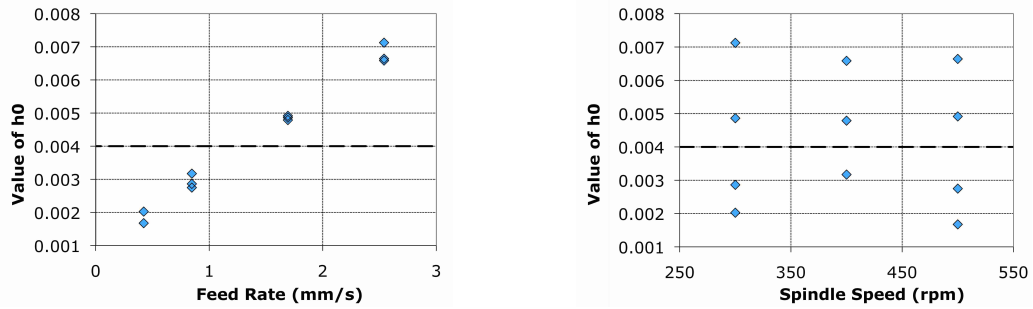

Figure 3-10: Optimal values of h_0 plotted against weld inputs. Dashed line is default value.

As Figure 3-10 indicates, the optimal h_0 is positively correlated to feed rate and not correlated to spindle speed. At this point is important to note the relationship between feed rate

and axial pressure. The axial pressure was not controlled in these experiments, and by plotting the axial pressure against the feed rate as shown in Figure 3-11, it is clear that the two are positively correlated.

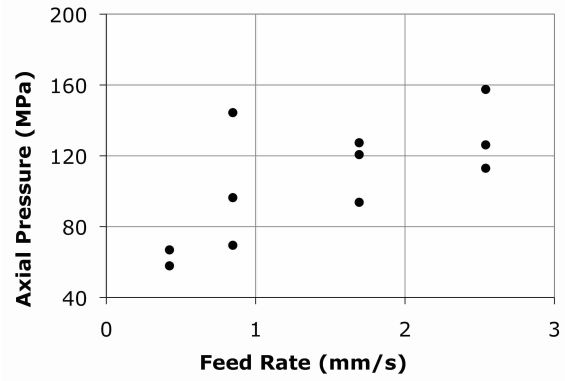

Figure 3-11: Axial pressure as a function of feed rate.

Thus, the positive correlation between h_0 and feed rate entails a positive correlation to axial pressure—this result has been well established in the literature of thermal contact resistance, where thermal contact resistance decreases with increased pressure [13]. However, it was surprising to see such strong linearity with feed rate. It is clear that using a constant value of h_0 = 0.004 cal/cm^2-s-K$^{1.25}$ would be inappropriate over a range of welds. Eqn (3-5) below gives the regression model for this parameter, where *FR* is the feed rate in mm/s.

$$h_0 = 8.122 \times 10^{-4} + (2.382 \times 10^{-3}) FR \tag{3-5}$$

It is important to note the high R^2 value of 0.99, as well as the high degree of statistical confidence in this regression model indicated by the closely spaced 95% confidence dashed lines. The fact that the unused welds had optimal h_0 values very close to the regression model's predicted values indicates that this regression model is valid.

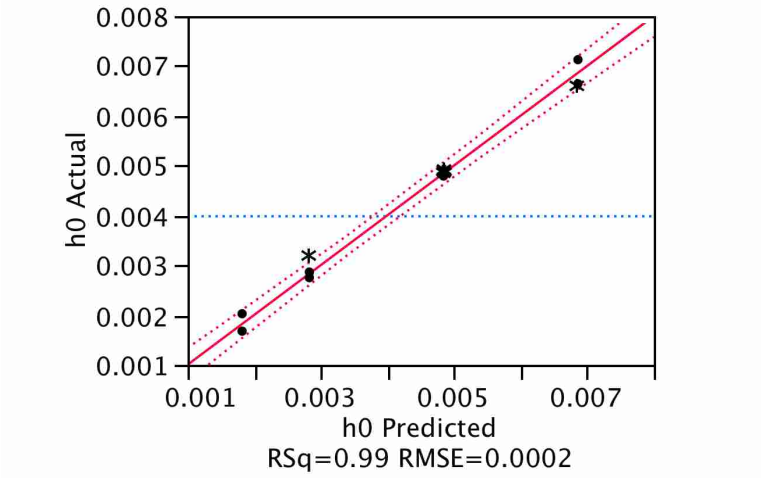

Figure 3-12: h_0 regression model. Welds not used denoted by *.

The result of this large variation in h_0 is that the convective coefficient below the tool is approximately equal to 400 W/m^2-K for the lowest feed rate welds (0.423 mm/s), while the highest feed rate welds (2.54 mm/s) have a corresponding h equal to 1500 W/m^2-K. Interestingly, these indicate more thermal contact resistance at the bottom of the plate than is expected. The available literature on thermal contact resistance indicates that stainless steel at high contact pressures (such as those experienced during friction stir welding) have h values ranging from 3,000 to 14,000 W/m^2-K [14].

3.5 Performance of model

Table 3-2 below is a summary of the regression equations. By incorporating the regression equations into the Penn State model, the model temperature error is decreased dramatically, with one weld being the exception, as shown in Figure 3-13. Using the regression equations also ensures greater consistency from weld to weld. The average model error using the default values is 257,000 with a weld-to-weld standard deviation of 169,000. By contrast, the model error using the regression equations averages 85,000 with a standard deviation of 47,000.

By using the optimal values for each weld, the model error averages 55,000 with a standard deviation of 24,000. With the exception of Weld No. 5, using the regression equations is nearly as good as using the best possible combination of parameter values (the optimal values).

Table 3-2: Regression equations and default values for the Penn State model parameters.

Model Parameter	*Default Value*	*Regression Equation*
Slip constant, δ_0	2.0	$\delta_0 = 9.1188 + 0.8973*FR - 0.0145*SS$
Friction constant, μ_0	0.45	None required – use default value
Mechanical efficiency, η	0.8	None required – use default value
Heat partition factor, f	0.41	$f = 0.6682 + 0.111*FR - 4.54 \times 10^{-4} *SS - 1.676 \times 10^{-3} *AP$
Heat transfer constant, h_0	0.004	$h_0 = 8.122e\text{-}4 + 2.382e\text{-}3*FR$

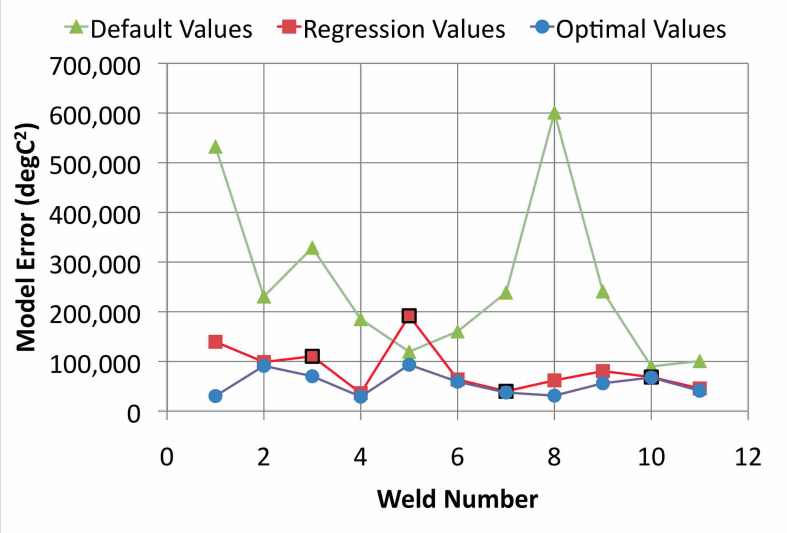

Figure 3-13: Model error by weld number using the default parameter values, the values obtained via the regression equations in Table 3-2, and the optimized values. The bolded squares indicate the regressed points.

In addition to computing workpiece temperatures, the Penn State model can predict torque at the tool-workpiece interface, material strain rates, and many other useful weld behaviors. Do the regression equations improve the Penn State model predictions in these other areas? In short, the answer is no. Figure 3-14 shows that the predicted torques (using both the

default and regression values) are significantly lower than the measured torque, and, other than in Welds 8-11, the trends do not match.

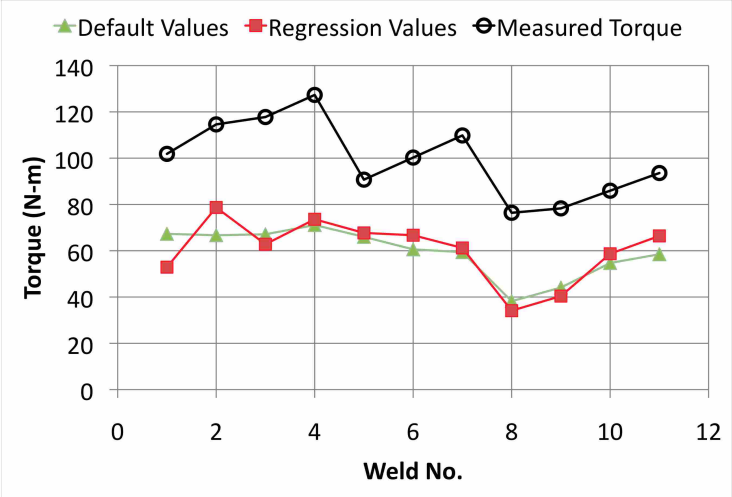

Figure 3-14: Measured spindle torque and predicted tool torque using the default and the regression values.

The total torque in the Penn State model, T_{total}, is calculated by

$$T_{total} = T_S + T_T + T_B \tag{3-6}$$

where T_S, T_T, and T_B, are the torques at the tool shoulder, threads (vertical part of probe), and base, respectively. The only one of these that is defined in the user-modifiable portion of the code is T_S, which is given through the force relationship

$$T_S = \sum\left[\left((1-\delta)\tau + \delta\mu P\right)rA\right] \tag{3-7}$$

where δ is the fraction of tool slip, τ is the shear stress, μ is the coefficient of friction, P is the axial pressure, r is the distance from the tool center, and A is the area of the discrete volume in contact with the tool shoulder region. As expected, T_S is the dominant source of torque. Using the optimal parameter values for Weld No. 6, T_S represents 93% of the total predicted torque of 66.7 N-m, while T_T and T_B represent 5 and 2 percent, respectively. Within T_S, there are two sources of torque: the first term, representing torque due to workpiece shear, and the second

term, representing torque due to Coulomb friction. Again, using the optimal parameter values for Weld No. 6, the first term only accounts for 0.7% of T_S.

The total torque may also be calculated via a power relationship as in

$$T_{total} = P/\omega = \frac{1}{f\omega}\left[(1/\eta)Q_{shear} + Q_{Coulomb}\right] \tag{3-8}$$

where P is the total power of the tool, ω is the rotational speed, f is the heat partition factor, η is the fraction of workpiece shear energy converted to heat, and Q_{shear} and $Q_{Coulomb}$ are the heat inputs (units of Watts) output by the Penn State model. Using this method, the total predicted torque for Weld No. 6 is 74.9 N-m. This is 12% higher than the force-based total torque that the model outputs. The cause of the inconsistency is not readily apparent.

The predicted thermo-mechanically affected zone (TMAZ) is not very accurate, either. Owen compared TMAZ geometry in a numerical model by plotting the contour of strain rate equal to 0.5 [8]. This is done for the Penn State model default and regression cases in Figure 3-15, which indicates that the Penn State model predicts an overly large TMAZ geometry (width and depth). Arora *et al* predicted TMAZ geometry by plotting the model's predicted iso-viscosity contour at 7×10^6 kg m^{-1} s^{-1} [7]. Performing the same analysis here yields TMAZ geometry nearly identical to that of Figure 3-15.

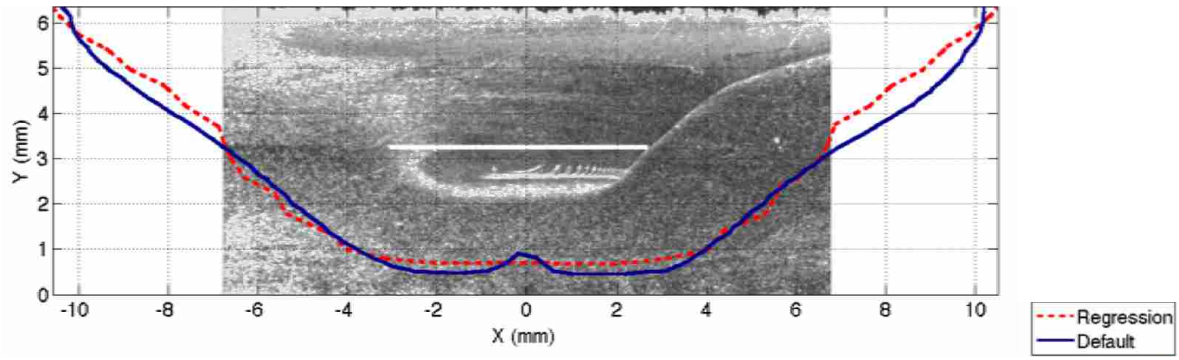

Figure 3-15: Predicted TMAZ geometry (default and regression values) plotted over the cross-section micrograph of Weld No. 2. The white bar above y = 3mm indicates thermocouple depth.

The Penn State model is unsuitable for predicting torque or TMAZ geometry in the welds Owen performed. Determining the cause of this modeling discrepancy is beyond the scope of this research; however, it is important to note that predicted torques and TMAZ geometries are no worse with the regression equations method, compared to the default parameters.

3.6 Conclusion

A method for determining previously unknown parameters in the Penn State model through optimization techniques and regression analysis has been discussed. Results were shown to lead to vastly improved predictions of workpiece thermal profiles in the mid-plane. Predictions of tool torque and TMAZ geometry were mostly unaffected.

Low spindle speed, high feed rate (or "cold") welds were shown to have higher heat partition factors and higher amounts of tool slip. Conversely, "hot" welds had less heat entering the workpiece and less tool slippage. Higher feed rate welds were shown to have higher heat transfer coefficients at the bottom surface of the plate, or put another way, higher feed rate welds were shown to have less thermal contact resistance at the bottom surface. The coefficient of friction and the mechanical efficiency were shown to have no correlation to feed rate, spindle speed, or axial pressure.

This research was supported by the Center for Friction Stir Processing, an NSF Industry/University cooperative research center.

4 COMPARISON OF A NUMERICAL MODEL OF THREE-DIMENSIONAL TEMPERATURE PROFILES TO EXPERIMENTAL RESULTS

4.1 Abstract

A numerical model of friction stir welding developed by T. DebRoy and others is optimized to fit two-dimensional temperatures collected in the mid-plane. However, three-dimensional temperature data indicates that the two-dimensionally optimized model does not sufficiently capture the thermal profiles in all three directions. Optimizing the model to fit the three-dimensional data does not yield acceptable results. Several potential sources for model improvement are identified, and it is demonstrated that adjusting the modeling of heat transfer through the bottom surface will lead to better thermal profiles. Predictions of torque and thermo-mechanical affected zone (TMAZ) geometry are unimproved.

4.2 Introduction

Friction stir welding (FSW) is a solid state welding process in which a rotating tool generates heat along the joint interface, resulting in the flow of plasticized material around the tool. Since 1991, when FSW was developed at TWI [1], many models (both analytical and numerical) have been documented [3]. Current work on FSW models holds promise in enabling researchers to predict weld temperatures, forces, residual stresses, and many other weld properties much more quickly than through experimentation alone. FSW modeling may also help researchers come to a better understanding of how the process works.

In this paper, a model of friction stir welding developed by T. DebRoy, R. Nandan, and others [4,6,7] is explored. The paper draws on previous work by Furse and Sorensen that sought to improve the predictive capabilities of the Penn State model by optimizing the model's predicted thermal profiles to match experimental temperatures obtained in the mid-plane of the plate [5]. The current work investigates whether this two-dimensional optimization approach yields good three-dimensional results. An experiment is documented wherein the requisite three-dimensional weld temperature data in 304L stainless steel is obtained.

4.3 Experimental procedure

A plate of 304L stainless steel having dimensions of 121.92 x 20.32 x 0.635 cm was embedded with fifty-six 0.032 inch grounded K-type thermocouples located according to Table A-1 in Appendix A. This approach followed the procedures outlined by Owen [8] and Dongfang [15], where the thermocouples are positioned and pressed into the workpiece via the assembly shown in Figure 4-1. The workpiece was friction stir welded to the same specifications as Owen's Weld No. 6: 400 rpm, 1.693 mm/s, and an axial force controlled to 33.3 kN.

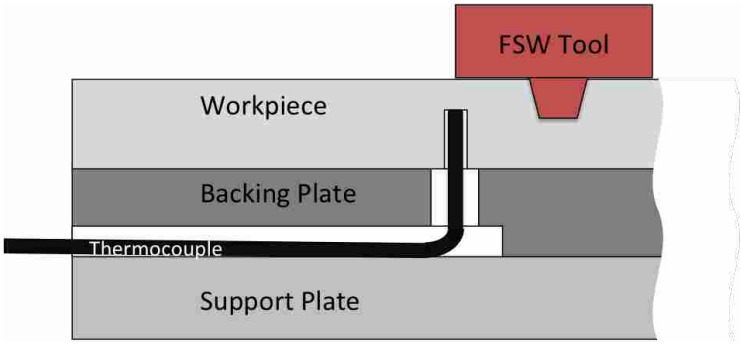

Figure 4-1: Thermocouple positioning assembly

The data from the 56 thermocouples was transformed from the time domain to the spatial domain relative to the tool axis by subtracting the thermocouple's absolute x position from the x position of the tool. This is possible due to assuming quasi-steady-state conditions around the tool. Owen showed that this assumption was valid for the weld conditions used in this study [8].

4.4 Two-dimensionally optimized results

The two-dimensionally optimized Penn State model temperatures are plotted in Figure 4-2 along with the experimental results from both Owen's study and the experiment documented in Section 4.3. The model was optimized to fit Owen's experimental temperatures, so naturally the model agrees well with his results in the mid-plane of z = 3.4 mm. However, when comparing the two-dimensional optimized model with the three-dimensional temperature data obtained, a few significant difficulties become apparent.

The first disagreement between model and experimental temperatures is that the model exaggerates the thermal asymmetry between advancing side (negative y) and retreating side (positive y). For example, Owen measured a difference of about 50 K in the peak temperatures between the thermocouples closest to the weld; the optimized model predicts a difference of more than 100 K. This asymmetry is clearly seen on the x = 0 plane, where temperatures of about 1400 K were measured on the retreating side. The model only predicted 1100 K – a very large error. The source of this discrepancy seems to be in the interfacial heat generation, given by eqn (2-5).

The model shows most of the heat being generated at the outer edges of the tool shoulder, overwhelmingly so on the advancing side. It may be that the model fails to adequately represent the mixing and transport of material, which would lead to more uniform temperatures across the

weld. Another alternative is that eqn (2-5) does not adequately represent heat generation in friction stir welding and that other phenomena are at work.

The second modeling disagreement is in the temperatures under the weld zone. In short, the model temperatures are far too high. On the plane x = 0, the two-dimensionally optimized model over-predicts the temperature at the bottom plate by 250 K. The experimental data indicates flatter, less vertical isotherms than the model predicts. This is seen in all the cross-section views of Figure 4-2. The source of this discrepancy may be due to the boundary condition at the bottom plate. It is treated as Newtonian cooling via eqn (2-7), where h is given by eqn (3-4). The justification for using eqn (3-4) is weak, as it is an empirical relation for an isothermal plate in free convection with air [11]. A contact resistance term would make more theoretical sense. This would be modeled as

$$k\left.\frac{\partial T}{\partial z}\right|_{bottom} = \frac{1}{R_{t,c}}\left(T - T_a\right) \tag{4-1}$$

where $R_{t,c}$ is the thermal contact resistance coefficient. To keep consistency with the rest of the Penn State model, $R_{t,c}$ would be expressed as $1/h$, with h having units of cal/s-m^2-K.

The third modeling disagreement is that the model temperature decreases too rapidly close to the shoulder on both the advancing and retreating sides. This may be due to the difference in modeling the tool geometry. The tool used in both welds (Owen's and the three-dimensionally instrumented) has the dimensions outlined in Figure B-1 in Appendix B. It has a convex shoulder which makes it difficult to tell where the contact with the workpiece ends. The Penn State model, on the other hand, represents the tool as shown in Figure 4-3, using five variables: the four shown and one variable indicating the thread pitch of the pin.

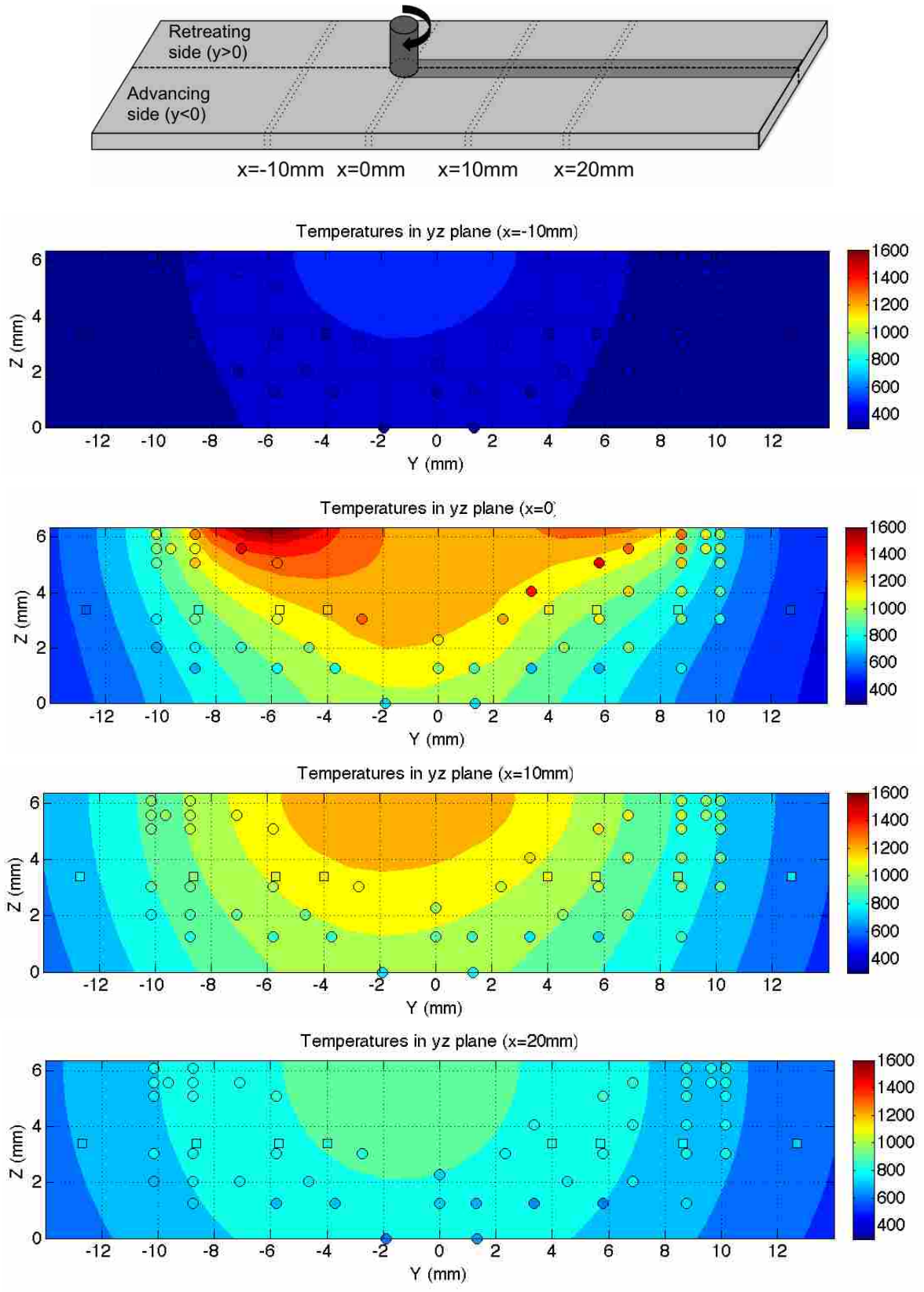

Figure 4-2: Cross-sectional views of model temperatures optimized to fit Owen's measurements (squares). This study's measurements (circles) are also shown. All temperatures in Kelvin.

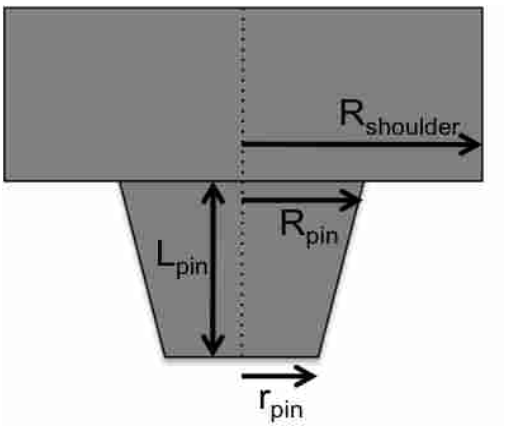

Figure 4-3: Penn State model tool geometry.

In modeling, the variables L_{pin}, R_{pin}, r_{pin}, and the thread pitch were all chosen from the tool dimensions in Appendix B. The variable $R_{shoulder}$ was chosen by measuring the physical weld width on the top surface of the plate after the weld was completed. The uncertainty in using this method and the simplified model geometry likely account for the difference in predicted and measured temperatures close to the shoulder radius.

Taken together, these three disagreements between the two-dimensionally optimized model and the actual measurements suggest that drawing three-dimensional conclusions from a two-dimensional optimization is inappropriate. It is now shown whether a three-dimensionally optimized model can adequately address these issues.

4.5 Three-dimensional optimization

4.5.1 Procedure

Optimization of the three-dimensional thermal profiles is performed similarly to previous efforts documented in earlier sections. The error function to be minimized is given by eqn (3-1) with the 77 optimization locations shown in Figure 4-4. The six monitoring locations at z = 0.34 were used in the two-dimensional optimization. Five additional cross-sectional locations have

been added. These locations were chosen to address the modeling issues mentioned in the above section, specifically the overly asymmetric temperatures from advancing to retreating side and the lack of a strong gradient under the weld.

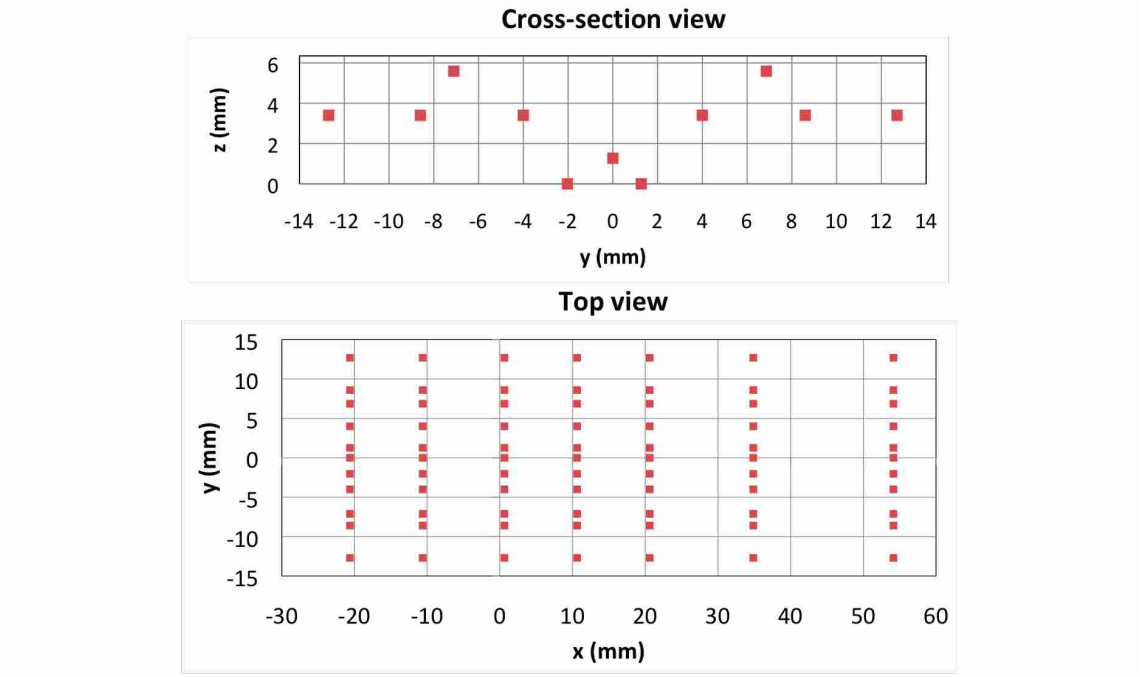

Figure 4-4: The 77 locations where the model error is calculated.

4.5.2 Results

Beginning with the default model parameter values documented in Table 3-2, the model error was quite large – 765,500 (or an average location error of about 100 K). The minimum model error that could be obtained through optimization was 553,400 (85 K), which did not seem to be much of an improvement, since two-dimensional optimization was able to reduce the average location error to 23 K. Optimal parameter values for both the two-dimensional and the

three-dimensional optimization are shown in Table 4-1. Most worthy of note is the increase in the heat partition factor, and the significant increase in the heat transfer constant h_0.

The resulting three-dimensionally optimized temperature contour plot from this set of model parameters is given in Figure 4-5. For the most part, the three-dimensionally optimized model does not address the issues raised in Section 4.4. There is still too much asymmetry, although this appears to have lessened somewhat. The temperatures under the weld are still too high, despite a drop in temperature at the bottom surface under the tool of almost 100 K. Lastly, the gradients near the tool shoulder are still too steep. The inability of the model to capture the thermal profiles indicates that any adjustment of the model parameters is insufficient.

Table 4-1: Optimal values for the Penn State model parameters for the 2-d and 3-d case.

Model Parameter	***Default Value***	***Two-dimensional Optimal Value***	***Three-dimensional Optimal Value***
Slip constant, δ_0	2.0	6.37	5.43
Friction constant, μ_0	0.45	0.45	0.45
Mechanical efficiency, η	0.8	0.8	0.8
Heat partition factor, f	0.41	0.45	0.51
Heat transfer constant, h_0 ($cal/cm^2\text{-}s\text{-}K^{1.25}$)	0.004	0.00479	0.0088

Interestingly, adjusting the model parameters *did* give the model sufficient flexibility to fit the mid-plane temperatures; however, this does not apply in the three-dimensional case. This suggests that there is a problem in the treatment of the boundary conditions, as hypothesized in Section 4.4. Specifically, the heat transfer at the bottom surface appears to be mistreated. There needs to be more heat transfer through the bottom of the plate both under the tool and behind it. This issue is treated in the following section.

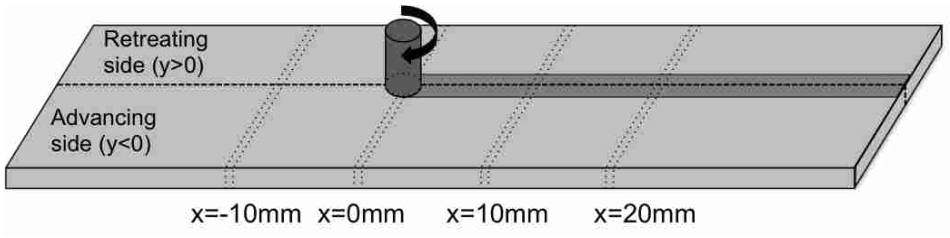

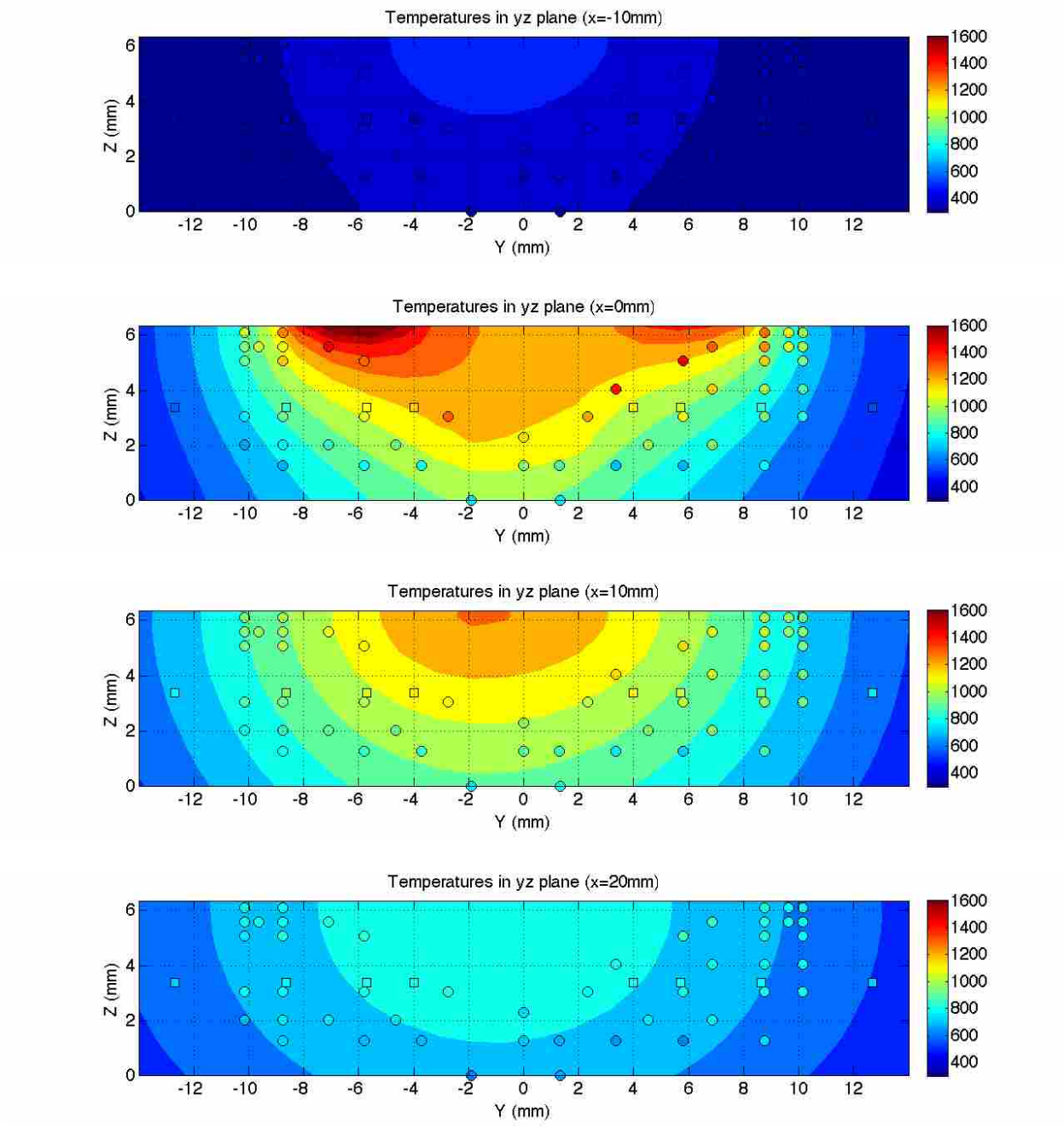

Figure 4-5: Cross-sectional views of model temperatures optimized to fit the locations shown in Figure 4-4. All temperatures in Kelvin.

4.5.3 Heat transfer at bottom surface

The poor modeling of temperature gradients in the z direction near the tool can be significantly improved by increasing the heat transfer coefficient at the bottom surface, as shown in Figure 4-6. In this figure, h_0 has been increased by an order of magnitude ($h_0 = 0.05$) and f has been increased to $f = 0.8$ to compensate for the additional heat lost though the bottom surface.

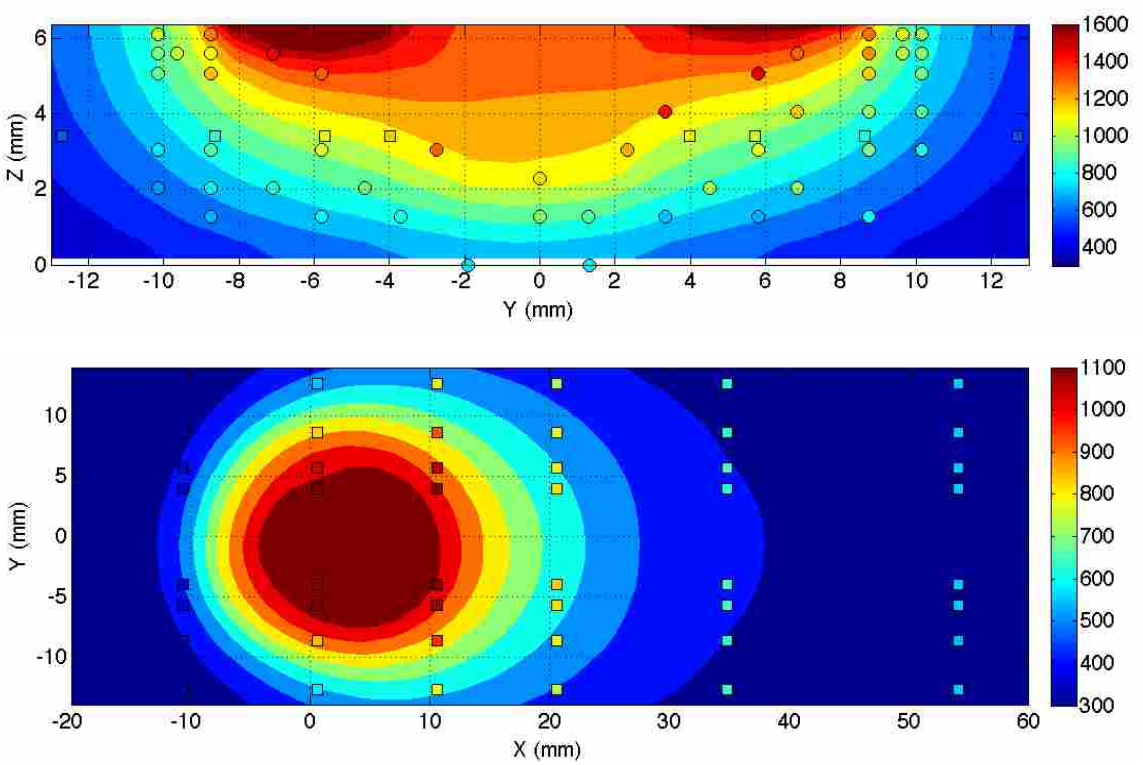

Figure 4-6: (Top) Improved cross-section model temperatures (x=0) by using a high h_0 value. (Bottom) Worsened gradients in x direction.

The temperature profiles near the tool are much more symmetric and the gradient in the z direction is appropriately steep. However, the gradients in the x direction are much worse than in the optimized case. The Penn State model can more accurately predict three-dimensional temperatures if the heat transfer boundary condition at the bottom surface is properly represented as a spatially-variable contact resistance term rather than a temperature-dependent convection

term as Shercliff and Colegrove suggest [3]. This is done using the setup shown in Figure 4-7, where the area directly under the tool shoulder has much lower contact resistance than the rest of the plate.

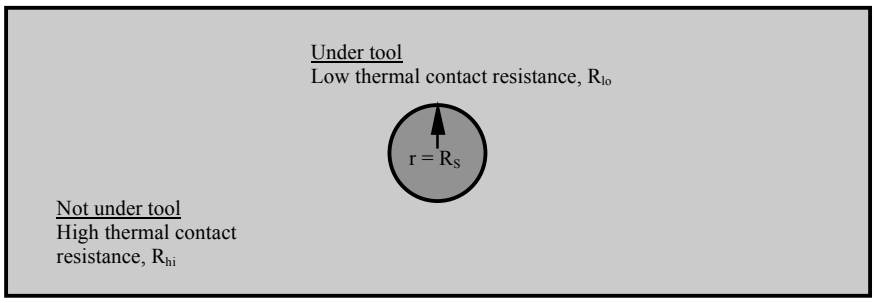

Figure 4-7: Spatially-variable contact resistance model for bottom surface.

The new thermal contact resistance modeling was optimized in the same manner as before. Table 4-2 shows the optimal values for the parameters. The *R* parameters, which have theoretical basis from eqn (4-2), have inverse units to the *h* values obtained in the previous method using eqn (3-4).

Table 4-2: Optimal values of the Penn State model parameters for the spatially variable thermal contact resistance method.

Model Parameter	***Optimal Value***
Slip constant, δ_0	3.024
Friction constant, μ_0	0.45 (used default)
Mechanical efficiency, η	0.8 (used default)
Heat partition factor, f	0.722
Resistance under tool, R_{lo} (cm^2-s-K-cal^{-1})	0.120
Resistance elsewhere, R_{hi} (cm^2-s-K-cal^{-1})	447.7

The resulting thermal profiles from this method are superior to those of the previous method, particularly in the z-direction. The x-direction thermal profiles are also acceptable, as

shown in Figure 4-8. However, because there is a step change in thermal contact resistance at the shoulder radius, the gradients appear somewhat warped. A transition zone from low to high resistance is more physically justifiable, and would probably correct the warped gradients.

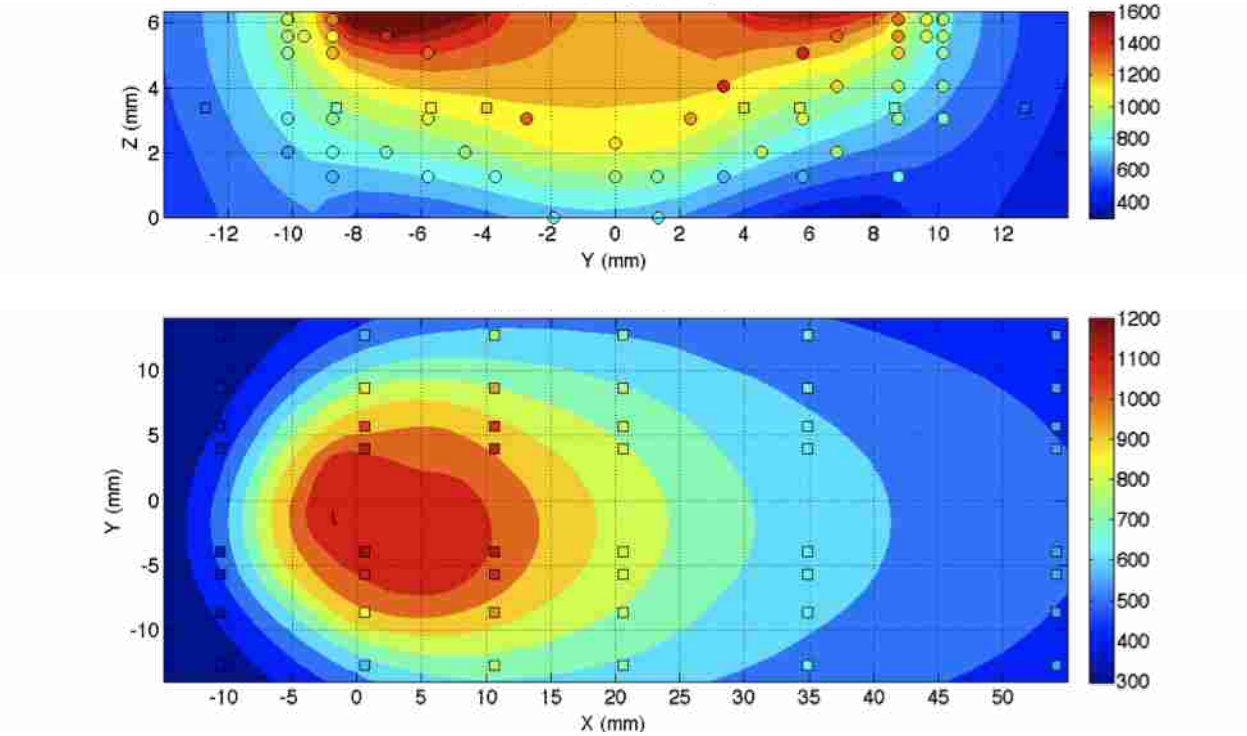

Figure 4-8: (Top) Cross-section (x=0) model temperatures (K) using spatially-variable contact resistance. (Bottom) Mid-plane (z=3.4mm) model temperatures (K) using spatially-variable contact resistance.

Despite the improved three-dimensional temperatures, the torque and TMAZ geometry predictions are still inadequate. The predicted torques using the spatially-variable contact resistance are 63.3 and 67.3 N-m using the force- and power-based methods detailed in Section 3.5, which are lower than the measured torque of approximately 100 N-m. The predicted TMAZ boundary (calculated per the procedure from Section 3.5) was mostly unaltered despite the drastic change in workpiece temperatures under the tool, as shown in Figure 4-9. That the boundary did not come closer to the tool plunge depth is troubling, since it was thought that the

depth of weld penetration might have been due to elevated model temperatures under the tool. The Penn State model may not be modeling material flow properly.

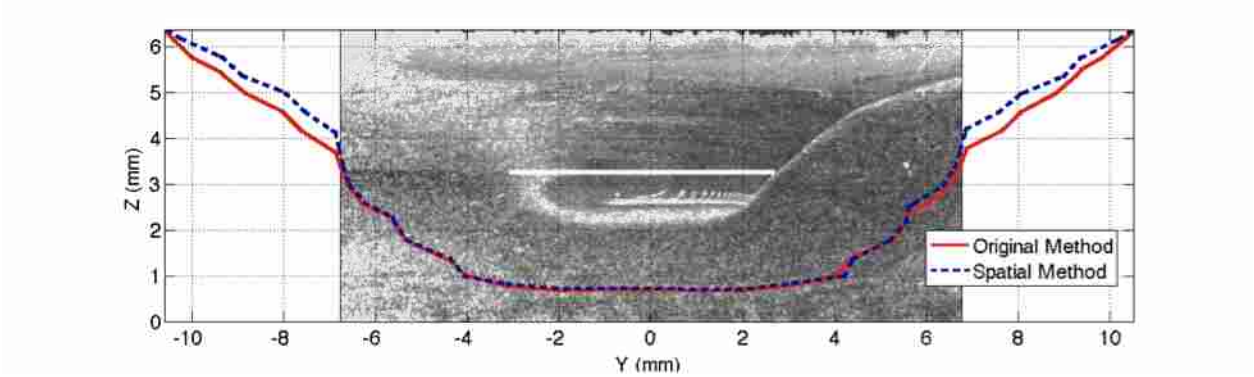

Figure 4-9: Predicted TMAZ for both approaches of heat transfer through the bottom surface.

4.6 Conclusion

Optimizing the Penn State model to temperatures in the mid-plane does not result in accurate three-dimensional thermal profiles. Optimizing to three-dimensional temperatures does not improve the model's three-dimensional predictions much either. The thermal profile is very sensitive to the heat transfer coefficient at the bottom face, and there is a trade-off in the current boundary condition scheme between accurate temperatures in the z direction and accurate temperatures in the x direction. Representing the bottom surface with a better theoretical relationship of thermal contact resistance improved thermal profiles in the z direction without the trade-off, but it did not improve predictions of torque or the TMAZ boundary.

5 RECOMMENDATIONS FOR FUTURE WORK

The modeling of heat transfer through the bottom of the workpiece is not based on good theory. Switching to a spatially-variable thermal contact resistance approach showed better agreement with measured temperatures; however, the step change in resistance (see Figure 4-7) led to strange behavior near the transition point. It is recommended to develop a transition zone between the high and low resistances. Since the Penn State model computes the pressure in each control volume, perhaps a relationship with pressure would be most reasonable, as contact resistance is highly correlated with pressure.

Optimization of the welds based on two-dimensional data may lead to good three-dimensional profiles if the heat transfer at the bottom surface is correctly addressed. This has not been attempted yet. If optimization of two-dimensional data still does not produce good three-dimensional profiles, more three-dimensionally instrumented welds at various feed rates and spindle speeds would need to be performed.

REFERENCES

[1] W. M. Thomas, E. D. Nicholas, J. C. Needham, M. G. Church, P. Templesmith, and C. Dawes: Int. Patent PCT/GB92/02203 and GB Patent 9125978-9, 1991.

[2] Nandan, R., DebRoy, T., & Bhadeshia, H.K.D.H., "Recent advances in friction-stir welding – Process, weldment structure, and properties." *Progress in Materials Science,* **53**, pp. 980-1023, 2008.

[3] Shercliff, H.R. & Colegrove, P.A., "Process Modeling" (Chapter 10). *Friction Stir Welding and Processing*, eds. Mishra, R.S. & Mahoney, M.W., ASM International, pp. 190-192, 2007.

[4] Nandan, R., Roy, G.G., Leinert, T.J. & DebRoy, T., "Numerical modelling of 3D plastic flow and heat transfer during friction stir welding of stainless steel." *Science and Technology of Welding and Joining*, **11(5)**, pp. 526-537, 2006.

[5] Furse, D., & Sorensen, C., "Optimization of a numerical model of three-dimensional heat transfer during friction stir welding of 304L stainless steel," *Fourth International Conference on Computational Methods and Experiments in Materials Characterisation*, pp. 23-31, 2009.

[6] Nandan, R., Roy, G.G., Leinert, T.J. & DebRoy, T., "Three-dimensional heat and material flow during friction stir welding of mild steel." *Acta Materialia*, **55**, pp. 883-895, 2007.

[7] Arora, A., Nandan, R., Reynolds, A.P. & DebRoy, T., "Torque, power requirement and stir zone geometry in friction stir welding through modeling and experiments." *Scripta Materialia*, **60**, pp. 13-16, 2009.

[8] Owen, B. "Two dimensional friction stir welding model with experimental validation," http://contentdm.lib.byu.edu/u?/ETD,585, 2006.

[9] Cowan, R.S. & Winer, W.O., "Frictional Heating Calculations," *ASM Handbook,* Vol. 18: Friction, Lubrication, and Wear Technology, pp. 39-44.

[10] Chao, Y.J., Qi, X. & Tang, W., "Heat transfer in friction stir welding – experimental and numerical studies." *ASME Journal of Manufacturing Science and Engineering*, 125, pp. 138-145, 2003.

[11] Schuhmann, R., *Metallurgical Engineering*, Addison-Wesley: Reading, eqn (7-31), 1952.

[12] Lawson, J. & Erjavec, J., *Modern Statistics for Engineering and Quality Improvement*, Duxbury: Pacific Grove, 2001.

[13] Incropera, F.P., & DeWitt, D.P., *Fundamentals of Heat and Mass Transfer*, 5th ed., John Wiley & Sons: New York, 2002.

[14] Fried, E., "Thermal Conduction Contribution to Heat Transfer at Contacts," in Tye, R.P., ed., *Thermal Conductivity*, Vol. 2, Academic Press, London, 1969.

[15] Dongfang, H., "Investigation of heterogeneity of FSW Inconel 718 coupled with welding thermal cycles," http://contentdm.lib.byu.edu/u?/ETD,1939, 2009.

APPENDIX A. THERMOCOUPLE PLACEMENT

The holes for the thermocouples were located via Table B-1, and were all drilled using a Size No. 65 bit. The x position is relative to the center of the alignment hole, the y position is relative to the centerline between the alignment holes (negative y is on the advancing side), and the z position is relative to the bottom of the plate (z = 0 at the plate bottom).

Table A-1: Location of thermocouple holes used in three-dimensional study.

Hole No.	*Channel-Switch*	*X (cm)*	*Y (cm)*	*Z (cm)*	*Hole No.*	*Channel-Switch*	*X (cm)*	*Y (cm)*	*Z (cm)*
1	8-1	15.12	0	0.127	29	1-3	60.48	1.008	0.4064
2	1-1	17.64	0.8568	0.127	30	9-3	60.48	-1.008	0.4064
3	9-1	17.64	-0.8568	0.127	31	2-3	65.52	0.8568	0.4064
4	2-1	20.16	0.5796	0.127	32	10-3	65.52	-0.8568	0.4064
5	10-1	20.16	-0.5796	0.127	33	3-3	68.04	0.6804	0.4064
6	3-1	22.68	0.3276	0.127	34	11-3	68.04	-0.7056	0.4064
7	11-1	22.68	-0.378	0.127	35	4-3	70.56	0.3276	0.4064
8	4-1	25.2	0.126	0.127	36	12-3	70.56	-0.378	0
9	12-1	25.2	-0.2016	0	37	5-3	73.08	1.008	0.508
10	5-1	27.72	0	0.2286	38	13-3	73.08	-1.008	0.508
11	6-1	32.76	1.008	0.2032	39	6-3	78.12	0.8568	0.508
12	13-1	32.76	-1.008	0.2032	40	8-3	78.12	-0.8568	0.508
13	7-1	37.8	0.8568	0.2032	41	7-3	80.64	0.5796	0.508
14	15-1	37.8	-0.8568	0.2032	42	15-3	80.64	-0.5796	0.508
15	1-2	40.32	0.6804	0.2032	43	1-4	83.16	1.008	0.5588
16	9-2	40.32	-0.7056	0.2032	44	9-4	83.16	-1.008	0.5588
17	2-2	42.84	0.4536	0.2032	45	2-4	85.68	0.9576	0.5588
18	10-2	42.84	-0.4536	0.2032	46	10-4	85.68	-0.9576	0.5588
19	3-2	45.36	0.126	0	47	3-4	88.2	0.8568	0.5588
20	11-2	45.36	-0.1764	0.2032	48	11-4	88.2	-0.8568	0.5588
21	4-2	47.88	1.008	0.3048	49	4-4	90.72	0.6804	0.5588
22	12-2	47.88	-1.008	0.3048	50	12-4	90.72	-0.7056	0.5588
23	5-2	52.92	0.8568	0.3048	51	5-4	93.24	1.008	0.6096
24	13-2	52.92	-0.8568	0.3048	52	13-4	93.24	-1.008	0.6096
25	6-2	55.44	0.5796	0.3048	53	6-4	95.76	0.9576	0.6096
26	8-2	55.44	-0.5796	0.3048	54	8-4	95.76	-0.9576	0.6096
27	7-2	57.96	0.2268	0.3048	55	7-4	98.28	0.8568	0.6096
28	15-2	57.96	-0.2772	0.3048	56	15-4	98.28	-0.8568	0.6096

APPENDIX B. TOOL DRAWING

The tool design used in all of the welds in this thesis is given in Figure B-1.

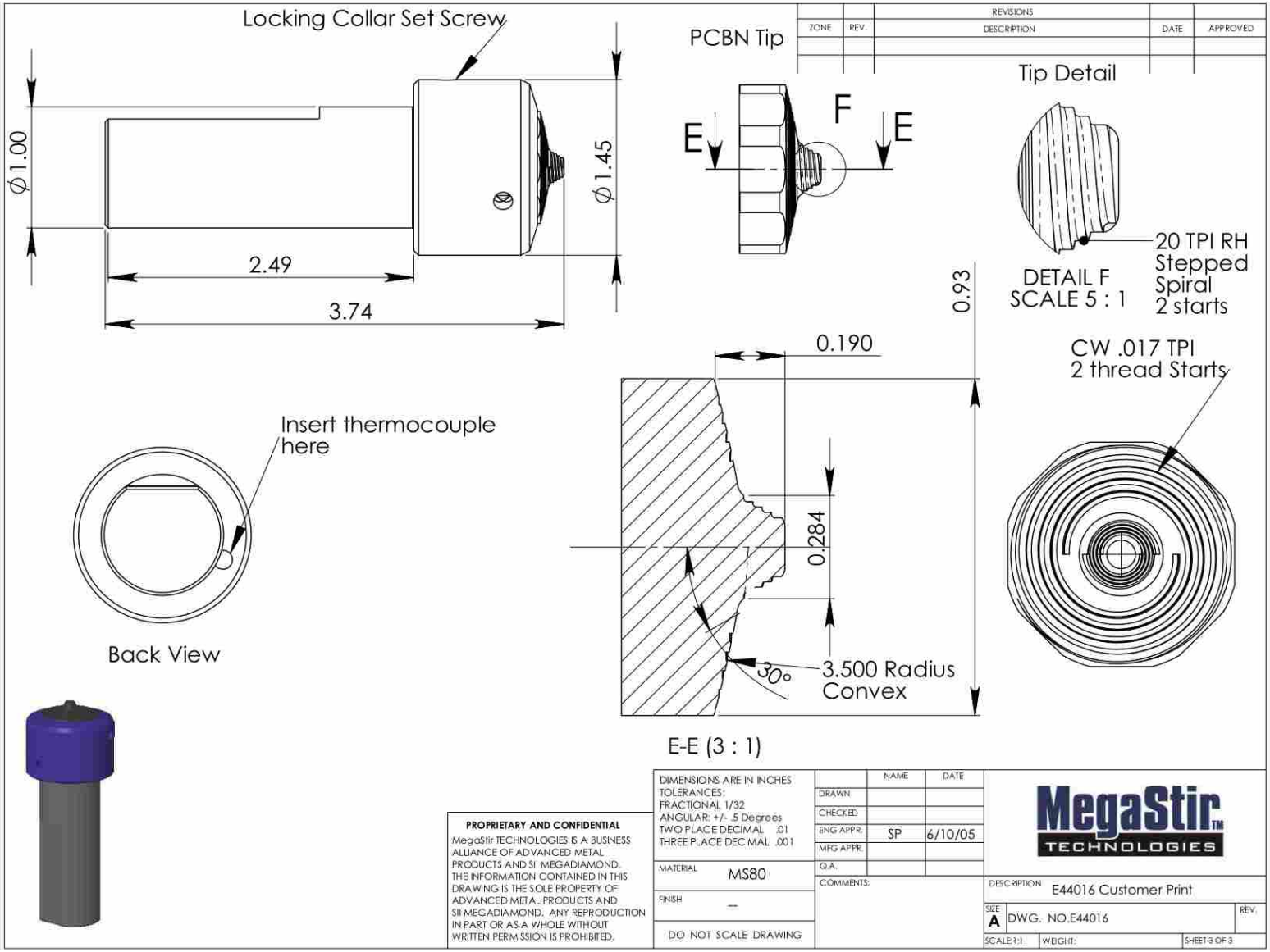

Figure B-1: FSW tool drawing No. E44016

APPENDIX C. CODE MODIFICATIONS

A few changes were made to the Penn State model user.for file. These changes are documented below.

- Restricted the `tau(i,j,k)` value (the workpiece shear strength in a discrete volume) to only be a positive number. Although the constitutive equation defining `tau` is not in a user-modifiable file, it was possible to write a line in user.for replacing negative values of `tau` with zero before this value was used in computing the frictional heat generation. This modeling change was associated with a "NaN error" which occurred during optimization that prevented the model from being fully optimized. The optimization and correlation of the Penn State model would have been impossible without this change.
- Commented the code at various locations for better understanding.
- Modified the section where tecmon.dat is written. The tecmon.dat output file was being appended to when the file should have been overwritten.

APPENDIX D. OPTIMIZATION SHELL FILE

In order to optimize the Penn State model, a shell file was written for OptdesX. The shell file updates the analysis variables (the Penn State model parameters) received from OptdesX, runs the Penn State model, parses the tecmon.dat output file for the temperatures at the specified locations, computes the model error, and returns the error to OptdesX. The following example is the PennState.sh shell file corresponding to Owen's Weld No. 1.

```
#! /bin/bash
##############################################################################################
# Script to use with OptDesX to optimize the Penn State Model                                #
# Created 10/02/2008 by Devin D. Furse, Esq.                                                 #
##############################################################################################

# Read in analysis variables (AV's) from OptdesX stored in Optin
# fric0 is first line of Optin, del0 is second line, etc.
{
read -r fric0
read -r del0
read -r htck1
read -r cf
read -r beta
read -r fracheat
read -r ubound
} <Optin

# Find/replace dummy variables with new AV's from OptdesX in user.txt to user.for
cat user.txt | sed -e "s/FRIC0/${fric0}/" -e "s/DEL0/${del0}/" -e "s/HTCK1/${htck1}/" -e
"s/CF/${cf}/g" -e "s/BETA/${beta}/g" -e "s/FRACHEAT/${fracheat}/g" -e "s/UBOUND/${ubound}/g" >
user.for

# Copy input.txt and new user.for file to Penn State's server
scp input.txt user3@fluid2.metsce.psu.edu:
scp user.for user3@fluid2.metsce.psu.edu:

# Access Penn State's server through SSH, compile and run model
# Note: Keys have been authenticated to automate login
ssh -t -t -l user3 fluid2.metsce.psu.edu <<-EOF
./compile.exe
./fsw.exe
logout
```

```
EOF

# Copy results from Penn State's server
scp -p user3@fluid2.metsce.psu.edu:tecmon.dat .
scp -p user3@fluid2.metsce.psu.edu:output001.txt .

# Measured temperatures of monitoring locations at given x values - corresponds to file "Graphs
E44016 in 304L 300rpm 1inmin.xls"
m11=452        # y = 8.89 cm
m12=657
m13=963
m14=894
m15=731
m16=593
m17=505
m21=463        # y = 9.2964 cm
m22=739
m23=1146
m24=989
m25=748
m26=591
m27=501
m31=490        # y = 9.76122 cm
m32=830
m33=1311
m34=1100
m35=770
m36=593
m37=501
m41=490        # y = 10.55878 cm
m42=830
m43=1320
m44=1093
m45=768
m46=593
m47=502
m51=460        # y = 11.0236 cm
m52=735
m53=1115
m54=971
m55=742
m56=589
m57=501
m61=443        # y = 11.43 cm
m62=634
m63=916
m64=867
m65=720
m66=588
m67=503

# Measured peak temperatures
m1=978         # y = 8.89 cm
m2=1161        # y = 9.2964 cm
m3=1314        # y = 9.76122 cm
m4=1330        # y = 10.55878 cm
m5=1130        # y = 11.0236 cm
m6=933         # y = 11.43 cm

# Predicted peak temperatures of columns (monitoring locations) in file tecmon.dat
```

```
sed -i '/TITLE/ d' tecmon.dat         # deletes TITLE header
sed -i '/VARIABLES/ d' tecmon.dat     # deletes VARIABLES header
awk 'max=="" || $2 > max {max=$2}END{print max}' FS=" " tecmon.dat > p
awk 'max=="" || $3 > max {max=$3}END{print max}' FS=" " tecmon.dat >> p
awk 'max=="" || $4 > max {max=$4}END{print max}' FS=" " tecmon.dat >> p
awk 'max=="" || $5 > max {max=$5}END{print max}' FS=" " tecmon.dat >> p
awk 'max=="" || $6 > max {max=$6}END{print max}' FS=" " tecmon.dat >> p
awk 'max=="" || $7 > max {max=$7}END{print max}' FS=" " tecmon.dat >> p
{
read -r p1
read -r p2
read -r p3
read -r p4
read -r p5
read -r p6
} <p

# Predicted temperatures at various x locations
awk 'NR==25{print $2}' tecmon.dat > p #line 25 = -20.62 mm
awk 'NR==25{print $3}' tecmon.dat >> p
awk 'NR==25{print $4}' tecmon.dat >> p
awk 'NR==25{print $5}' tecmon.dat >> p
awk 'NR==25{print $6}' tecmon.dat >> p
awk 'NR==25{print $7}' tecmon.dat >> p
awk 'NR==33{print $2}' tecmon.dat >> p       #line 33 = -10.62 mm
awk 'NR==33{print $3}' tecmon.dat >> p
awk 'NR==33{print $4}' tecmon.dat >> p
awk 'NR==33{print $5}' tecmon.dat >> p
awk 'NR==33{print $6}' tecmon.dat >> p
awk 'NR==33{print $7}' tecmon.dat >> p
awk 'NR==42{print $2}' tecmon.dat >> p       #line 42 = 0.625 mm
awk 'NR==42{print $3}' tecmon.dat >> p
awk 'NR==42{print $4}' tecmon.dat >> p
awk 'NR==42{print $5}' tecmon.dat >> p
awk 'NR==42{print $6}' tecmon.dat >> p
awk 'NR==42{print $7}' tecmon.dat >> p
awk 'NR==50{print $2}' tecmon.dat >> p       #line 50 = 10.62 mm
awk 'NR==50{print $3}' tecmon.dat >> p
awk 'NR==50{print $4}' tecmon.dat >> p
awk 'NR==50{print $5}' tecmon.dat >> p
awk 'NR==50{print $6}' tecmon.dat >> p
awk 'NR==50{print $7}' tecmon.dat >> p
awk 'NR==58{print $2}' tecmon.dat >> p       #line 58 = 20.62 mm
awk 'NR==58{print $3}' tecmon.dat >> p
awk 'NR==58{print $4}' tecmon.dat >> p
awk 'NR==58{print $5}' tecmon.dat >> p
awk 'NR==58{print $6}' tecmon.dat >> p
awk 'NR==58{print $7}' tecmon.dat >> p
awk 'NR==63{print $2}' tecmon.dat >> p       #line 63 = 34.86 mm
awk 'NR==63{print $3}' tecmon.dat >> p
awk 'NR==63{print $4}' tecmon.dat >> p
awk 'NR==63{print $5}' tecmon.dat >> p
awk 'NR==63{print $6}' tecmon.dat >> p
awk 'NR==63{print $7}' tecmon.dat >> p
awk 'NR==65{print $2}' tecmon.dat >> p       #line 65 = 54.14 mm
awk 'NR==65{print $3}' tecmon.dat >> p
awk 'NR==65{print $4}' tecmon.dat >> p
awk 'NR==65{print $5}' tecmon.dat >> p
awk 'NR==65{print $6}' tecmon.dat >> p
awk 'NR==65{print $7}' tecmon.dat >> p
```

```
{
read -r p11
read -r p21
read -r p31
read -r p41
read -r p51
read -r p61
read -r p12
read -r p22
read -r p32
read -r p42
read -r p52
read -r p62
read -r p13
read -r p23
read -r p33
read -r p43
read -r p53
read -r p63
read -r p14
read -r p24
read -r p34
read -r p44
read -r p54
read -r p64
read -r p15
read -r p25
read -r p35
read -r p45
read -r p55
read -r p65
read -r p16
read -r p26
read -r p36
read -r p46
read -r p56
read -r p66
read -r p17
read -r p27
read -r p37
read -r p47
read -r p57
read -r p67
} <p

# Calculate average peak temperature error
PeakErr=$(echo "scale=9;($p1-$m1)^2+($p2-$m2)^2+($p3-$m3)^2+($p4-$m4)^2+($p5-$m5)^2+($p6-$m6)^2"
|bc)

# Calculate error function and write to Optout
Error=$(echo "scale=9;($p11-$m11)^2+($p12-$m12)^2+($p13-$m13)^2+($p14-$m14)^2+($p15-
$m15)^2+($p16-$m16)^2+($p17-$m17)^2+($p21-$m21)^2+($p22-$m22)^2+($p23-$m23)^2+($p24-
$m24)^2+($p25-$m25)^2+($p26-$m26)^2+($p27-$m27)^2+($p31-$m31)^2+($p32-$m32)^2+($p33-
$m33)^2+($p34-$m34)^2+($p35-$m35)^2+($p36-$m36)^2+($p37-$m37)^2+($p41-$m41)^2+($p42-
$m42)^2+($p43-$m43)^2+($p44-$m44)^2+($p45-$m45)^2+($p46-$m46)^2+($p47-$m47)^2+($p51-
$m51)^2+($p52-$m52)^2+($p53-$m53)^2+($p54-$m54)^2+($p55-$m55)^2+($p56-$m56)^2+($p57-
$m57)^2+($p61-$m61)^2+($p62-$m62)^2+($p63-$m63)^2+($p64-$m64)^2+($p65-$m65)^2+($p66-
$m66)^2+($p67-$m67)^2" | bc)
echo $p1 > Optout
echo $p2 >> Optout
```

```
echo $p3 >> Optout
echo $p4 >> Optout
echo $p5 >> Optout
echo $p6 >> Optout
echo $m1 >> Optout
echo $m2 >> Optout
echo $m3 >> Optout
echo $m4 >> Optout
echo $m5 >> Optout
echo $m6 >> Optout
echo $Error >> Optout
echo $PeakErr >> Optout
```